C.P. No. 295
(18,181)
A.R.C. Technical Report

C.P. No. 295
(18,181)
A.R.C. Technical Report

MINISTRY OF SUPPLY

AERONAUTICAL RESEARCH COUNCIL

CURRENT PAPERS

The Direction of Flow in the Laminar Boundary Layer on an Infinite Yawed Cylinder

By

K. D. P. Sinha, M.Sc.

of the Engineering Laboratory, University of Cambridge

LONDON . HER MAJESTY'S STATIONERY OFFICE

1956

Price 5s 6d net

C.P. No. 295

The Direction of Flow in the Laminar Boundary Layer on an Infinite Yawed Cylinder

- By -
K. D. P. Sinha, M.Sc.
Engineering Laboratory, University of Cambridge

Communicated by Prof. W. A. Mair

28th January, 1956

SUMMARY

In a previous report[11] the exact solutions of the spanwise laminar boundary layer on an infinite yawed cylinder with distributed suction, were given for all the known exact solutions of the chordwise boundary layer for the chordwise velocity distribution, $U = U_o x^m$.

In the present report the same class of exact solutions has been used to investigate the direction of the velocity vector, and hence the curvature of the streamlines and the secondary flow. In the analysis the curvature of the edge streamline has been taken into account. The investigation includes both positive and negative pressure gradients and a wide range of distributed suctions.

It is found that:

(1) The primary flow profiles always lie between the chordwise and spanwise boundary layer profiles, and the secondary flow profiles always have a point of inflexion.

(2) Secondary flows are opposite in direction for positive and negative pressure gradients and are a maximum when the edge streamline makes 45° with the chordwise direction.

(3) An adverse pressure gradient produces a more powerful secondary flow than a favourable pressure gradient of the same numerical strength.

(4) A pressure gradient of any sign increases the secondary flow, and distributed suction decreases it.

Secondary flow instability has been considered in terms of the Reynolds number of the secondary flow (Owen's criterion) and curves of the ratio of the secondary flow Reynolds number to the primary flow Reynolds number are presented for various inclinations of the edge streamline to the chordwise direction.

Contents/

Contents

1./

1. Introduction

The boundary layer over an infinite yawed cylinder has become of considerable interest in recent years, because many modern aircraft have sweptback wings. The boundary layer on an infinite sweptback wing is three-dimensional in nature and presents some special features which have an important bearing on the realisation of laminar flow. The present investigation was completed before the papers listed in References Nos. 1, 2, 3, 4, 5 and 6, were available to the author. Some of the conclusions are similar but the approach is different, and the work is limited to a particular class of solutions.

In 1951 Gray[1] observed, in a visual determination of transition in flight, that sweepback had a profound destabilising effect on a laminar boundary layer near the nose of a wing. Further flight tests confirmed that the instability started in the form of striations with their axes along the wind, spaced at distinct intervals, and having the appearance of the Görtler vortices found in flow over a concave surface.

Theoretical explanations of the above phenomena were given independently by Squire[2], by Owen and Randall[3], and by Stuart[4]. They state that the instability is associated with a point of inflexion in the velocity profile through the boundary layer in a direction normal to that of the edge streamline. This extra flow normal to the main flow was called the 'secondary flow', and is caused by the curvature of the streamlines in the tangent planes parallel to the surface.

The use of a leading edge suction slot to reduce this instability was suggested by Gray[5], and the calculations of Owen and Randall[6] for constant suction velocities showed that suction would reduce the secondary flow and thereby the instability caused by it.

For investigating this secondary flow instability, Owen and Randall[3] assumed, for simplicity, that the edge streamline is straight in the direction of the free stream, although they noted that near the leading edge the streamline outside the boundary layer is highly curved. The assumption is therefore open to criticism because the instability was investigated near the leading edge. The present treatment is not restricted by any such assumption, and furthermore also deals with the case of a positive pressure gradient, for which there has been no previous detailed investigation.

To determine both the direction of flow and the secondary flow, in the boundary-layer on an infinite yawed cylinder, it is necessary first to find the velocity components at any point of the boundary layer. The velocity profiles used for this purpose have been taken from the exact solutions of the chordwise and spanwise boundary-layer equations, with the velocity distribution $U = U_o x^m$ at the edge of the chordwise boundary layer. For zero suction the chordwise and spanwise solutions with 'similar profiles' have been given by Hartree[7] and by Cooke[8] respectively. With distributed suction and 'similar profiles', the chordwise solutions were given by Schlichting and Bussmann[9] for the stagnation flow ($m = 1$), and by Thwaites[10] for positive pressure gradients ($m < 0$). The corresponding exact solutions for the spanwise flow were obtained by the author[11] in an earlier paper.

2./

2. Notation

x, y, z	co-ordinates measured in the chordwise direction, spanwise direction, and normal to the surface respectively
u, v, w	velocity components in x, y and z directions respectively
U	chordwise velocity at the edge of the boundary layer
V_o	spanwise velocity in the free stream
w_o	normal suction velocity on the surface
w_1	normal velocity at the edge of the layer
η	a non-dimensional quantity $= \left(\frac{U}{\nu x}\right)^{\frac{1}{2}} z$
ν	kinematic viscosity $= \mu/\rho$
m	index in the relation $U = U_o x^m$
$f(\eta)$	a function defined by $\psi = (\nu\, Ux)^{\frac{1}{2}} f(\eta)$
$f'(\eta) = \frac{u}{U}$	non-dimensional chordwise velocity
Y	a non-dimensional parameter $= [\frac{1}{2}(m+1)]^{\frac{1}{2}}\eta$
β	semi-wedge angle $= \frac{2m}{m+1}$
$F(Y) = [\frac{1}{2}(m+1)]^{\frac{1}{2}} f'(\eta)$	
$K = F_o$	value of $F(Y)$ on the boundary
$g'(\eta) = G'(Y) = \frac{v}{V_o}$	non-dimensional spanwise velocity
γ	angle of sweep
θ	inclination of the plane of resultant flow with the chordwise direction
ϕ	inclination of the resultant velocity with the Z-axis
$\theta_e = \tan^{-1}\frac{V_o}{U}$	inclination of the edge-streamline with the chordwise direction
δ	boundary-layer thickness
u_1	velocity component of the primary flow in the direction of the edge streamline
v_1	velocity component of the secondary flow in the plane normal to the direction of the edge-streamline
$U_1 = \sqrt{V_o^2+U^2}$	resultant velocity at the edge of the boundary layer

$\left|\frac{u_1}{U_1}\right|$

$\frac{u_1}{U_1}$ non-dimensional velocity of the primary flow

$\frac{v_1}{U_1}$ non-dimensional velocity of the secondary flow

$\chi = \frac{|v_1|_{max}\,\delta}{\nu}$ = Reynolds number for the secondary flow

$\chi_1 = \frac{U_1\,\delta}{\nu}$ = Reynolds number for the primary flow

---

3. Direction of Flow

Before determining the actual direction of flow in the boundary layer, let us suppose that the y-axis is the axis of the cylinder, the x-direction at any point is tangential to the boundary and normal to the axis of the cylinder, and the z-direction at any point is normal to the boundary. Then, u, v and w, are the velocity components parallel to x, y and z respectively. The axis of the cylinder is supposed to be infinite in length, so all boundary-layer quantities will be independent of the y-co-ordinate, and the flow pattern across all sections of the cylinder normal to the axis will be the same.

If θ is the angle which the vertical plane through the resultant velocity vector makes with the x-direction, and ϕ is the inclination of the resultant velocity with the z-direction then

$$\tan\theta = \frac{v}{u}, \qquad \ldots\ldots(1)$$

$$\tan\phi = \frac{\sqrt{u^2 + v^2}}{w}, \qquad \ldots\ldots(2)$$

and the direction-cosines of the velocity vector are given by

$$\cos\theta \sin\phi, \quad \sin\theta \sin\phi, \quad \text{and} \quad \cos\phi \qquad \ldots\ldots(3)$$

The value of w at the edge of the layer is usually small, so that ϕ is nearly 90°, and the resultant flow at the edge of the layer is almost parallel to the boundary.

3.1 Direction of flow with 'similar profiles' $U = U_o x^m$.

For zero suction the solutions of this class of velocity distributions were obtained by Hartree (chordwise solutions) and Cooke (spanwise solutions). The stagnation flow with suction was investigated by Schlichting and Bussmann[9], and the corresponding spanwise solution was obtained by the author[11]. For positive pressure gradients Thwaites[10] has obtained a large number of solutions with different suctions for the chordwise layer, and the corresponding solutions for the spanwise layer have been obtained by the author[11]. These solutions will provide the velocity components to determine the direction-cosines of the velocity vector by the relation (3).

The direction parameter 'θ' can be calculated from the relation

$$\tan\theta = g'/f' \tan\theta_e, \qquad \ldots\ldots(4)$$

where/

where $g'(\eta) = \frac{v}{V_o}$, $f'(\eta) = \frac{u}{U}$, and $\tan \theta_e = \frac{V_o}{U}$

On the boundary, $$\tan \theta = \frac{g''(0)}{f''(0)} \tan \theta_e , \qquad \ldots\ldots(5)$$

and at the edge of the layer $$\tan \theta = \tan \theta_e \qquad \ldots\ldots(6)$$

Since the variables in the expression for $\tan \theta$ are functions of the pressure gradient, the suction, and the direction of flow at the edge of the layer (θ_e), the calculation of θ can be considered as follows.

(i) Zero pressure gradient $(m = 0)$. In this case the chordwise and spanwise velocity profiles are identical for all suctions, and θ_e is always equal to the angle of yaw (i.e., γ), hence at all points in the boundary layer θ is equal to γ.

(ii) Positive pressure gradient $(m < 0)$. In this case g' is always greater than f' for all values of η except at the boundary and at the edge of the boundary layer. At the boundary $g''(0)$ is greater than $f''(0)$, for all suctions, as will be clear from the Figure 11 of Reference 11. Therefore from (4) and (5),

$$\tan \theta > \tan \theta_e \qquad \ldots\ldots(7)$$

for all suctions and for all values of η in the boundary layer. The maximum value of θ is θ_b, attained at the boundary, and the minimum value is θ_e, at the edge of the boundary layer. Thus,

$$\theta_b \geq \theta \geq \theta_e \qquad \ldots\ldots(8)$$

(iii) Negative pressure gradient $(m > 0)$. In this case g' is less than f', for all suctions, and for all values of η except on the boundary and at the edge of the boundary layer, where the boundary conditions give $g' = f'$. At the boundary $g''(0)$ is always less than $f''(0)$, as will be clear from Fig.13 of Reference 11. Therefore from (4) and (5),

$$\theta_b \leq \theta \leq \theta_e \qquad \ldots\ldots(9)$$

It is seen that the maximum value of θ is attained at the edge of the boundary layer and the minimum value on the boundary.

These results obtained for the variation of θ are very important, because they determine the lateral curvatures of the streamlines in the boundary layer and thereby the secondary flows and the instability caused by them on sweptback wings.

The other parameter ϕ is only of theoretical interest and is not so important for practical applications.

3.2 Examples

(a) Flat plate $(m = 0)$. In this case θ is always equal to γ, and the direction of flow at all points in the boundary layer is the same as that of the free stream. Values of ϕ have been calculated and the results are given in Tables 1, 2 and 3.

(b)/

(b) Flow near the stagnation line ($U = U_o x$). The parameter θ is calculated from the relations (4) and (5) for a wide range of suctions, θ_e and η, and the results are given in Table 4.

The parameter ϕ can be calculated from the relations

$$\tan \phi = \frac{f'}{\frac{w}{U}\cos\theta},$$

and

$$\frac{w}{U} = -\frac{f}{\sqrt{\frac{U_o}{\nu}x}} \qquad \ldots\ldots(10)$$

It is clear from (10) that the w-component is always negative throughout the boundary layer, even if it has the initial value zero on the boundary in the case of zero suction. Table (a) below gives the extreme values of the w-component, w_o on the boundary and w_1 at the edge of the layer.

Table (a)

K	$w_o/(U_o\nu)^{\frac{1}{2}}$	$w_1/(U_o\nu)^{\frac{1}{2}}$
0	0	-3.252
0.5	-0.5	-3.058
1.095	-1.095	-3.500
1.9265	-1.9265	-4.0
2.664	-2.664	-4.50

Thus w_1 is always numerically greater than w_o. Therefore, since θ is always acute, ϕ will always be in the second quadrant ($90° \leq \phi \leq 180°$).

(c) The case $\beta = -1$, $U = U_o x^{-\frac{1}{3}}$. The value of θ was calculated for a number of values of the parameters and the results are presented in Table 5. The value of ϕ may be calculated from the relations

$$\tan \phi = \frac{F'}{\frac{w}{U}\cos\theta}$$

and

$$\frac{w}{U} = -\frac{1}{\sqrt{3}} R_x^{-\frac{1}{2}} (F - 2YF'), \qquad \ldots\ldots(11)$$

where

$$F = \frac{1}{\sqrt{3}} f, \quad F' = f' \quad \text{and} \quad Y = \frac{1}{\sqrt{3}} \eta.$$

Equation (11) does not show directly whether w will be positive or negative in the boundary layer. The values w_o and w_1 respectively on the boundary and at the end of the boundary-layer are shown below

Table(b)/

Table (b)

K	$w_o/(Uv/3x)^{\frac{1}{2}}$	$w_1/(Uv/3x)^{\frac{1}{2}}$
1.414	-1.414	0
1.421	-1.421	-0.14
1.437	-1.437	-0.25
1.500	-1.50	-0.50
1.554	-1.554	-0.64

Thus ϕ always lies in the second quadrant (90° to 180°), since $\tan\phi$ is always negative except in the separation case ($K = 1.414$), where $\tan\phi = \infty$ at the edge of the boundary layer.

4. Streamlines in the Boundary Layer

The flow in the boundary layer on an infinite yawed cylinder is three-dimensional in nature, as is evident from relations (1), (2) and (3). The introduction of distributed suction only alters one boundary condition (at the wall) and does not change the general character of the flow. Each streamline may be considered as having two kinds of curvature at any point, viz., (1) the lateral curvature due to the variation in θ from point to point and (2) the normal curvature due to the variation of ϕ in the boundary layer. There is an exception in the case of the flat plate, where the streamlines are plane-curves in the plane $\theta = \gamma$ (angle of yaw), and have only normal curvature.

In principle, it is possible to construct streamlines with soft wires or any other similar solid material if the values of θ and ϕ are given at all points in the boundary layer at a particular level, but it is difficult to represent the three-dimensional curves on two-dimensional paper. Several authors, e.g., Sears,[15] Wild,[16] and Rott and Crabtree[17] have considered the streamlines on yawed infinite cylinders with zero suction, but they have only given the actual streamlines of the flow nearest to the boundary where the w-component vanishes. They found that the remaining projected streamlines lie between the two extremes, the streamline nearest to the boundary, and the streamline at the edge of the boundary layer.

When distributed suction is applied, the streamlines change in curvature. On the porous boundary, $\phi = 180°$ and the streamlines are the normals directed towards the boundary. In the neighbourhood of the porous boundary, the streamlines are curved in three dimensions, since the w-component does not vanish. The streamlines are of the same general nature at the edge of the boundary layer, if the w-component is not negligible there. It is always true that the remaining streamlines lie between the two extreme ones in plan view, since all values of θ for positive or negative pressure gradients lie between the extreme values θ_b and θ_e (Tables 4 and 5).

The projection of the streamlines on a plane parallel to the wall is given by the equation

$$\frac{dy}{dx} = \frac{v}{u}, \qquad \ldots\ldots(12)$$

which/

which becomes
$$\frac{dy}{dx} = \frac{g'}{f'} \tan \gamma \, x^{-m} \qquad \ldots\ldots(13)$$

for 'similar profiles' $U = U_o x^m$ at the edge of the chordwise boundary-layer.

For the boundary streamline the equation (13) becomes

$$\frac{dy}{dx} = \frac{g''(0)}{f''(0)} \tan \gamma \, . \, x^{-m} \qquad \ldots\ldots(14)$$

and for the edge of the boundary-layer it reduces to

$$\frac{dy}{dx} = \tan \gamma \, x^{-m} \qquad \ldots\ldots(15)$$

If y_b and y_e are the values of y at the two extreme streamlines, for a given value of x, then

$$\frac{y_b}{y_c} = \frac{g''(0)}{f''(0)} \qquad \ldots\ldots(16)$$

As already mentioned, the values of y on the remaining streamlines, for the same value of x, must all be between y_b and y_e.

4.1 Streamlines in some special cases

(i) Flat plate.- In this case $m = 0$, and $g''(0)$ becomes equal to $f''(0)$. Hence, $y_b = y = y_c$ for all values of x and all the streamlines of a particular section along the stream, projected on a plane parallel to the boundary, lie in the same straight line in that plane.

(ii) Flow near the stagnation line.- In this case $m = 1$, and the extreme streamlines in plan view will be given by

$$y_b = \frac{g''(0)}{f''(0)} \tan \gamma \log x/\epsilon,$$

and $\qquad \ldots\ldots(17)$

$$y_e = \tan \gamma \log x/\epsilon,$$

respectively, on the boundary and at the edge of the boundary layer. ϵ is a constant of zero order but is not exactly zero. This constant ϵ has been introduced to avoid a singularity at the leading edge ($x = 0$) and the streamlines will be given from $x = \epsilon$, which is extremely near the leading edge.

Any other streamline between the two extreme streamlines in plan view will be given by

$$y = A \tan \gamma \log x/\epsilon, \qquad \ldots\ldots(18)$$

where A is a constant between $\frac{g''(0)}{f''(0)}$ and unity.

Therefore/

Therefore, the projections of the streamlines on the boundary for the stagnation flow, are logarithmic curves, both for the solid and for the porous boundaries. This is in agreement with the finding of Rott and Crabtree[17], who considered only the case of zero suction.

Effect of suction on the ratio y_b/y_e. Since the pressure gradient is fixed, this ratio is affected only by suction; and it increases with the suction parameter K. Moreover, this ratio is always less than unity, and tends to approach unity for very large suctions, as shown below.

Table (c)

K	$\frac{y_b}{y_e} = \frac{g''(0)}{f''(0)}$
0	0.4628
0.5	0.5984
1.095	0.7188
1.9265	0.8221
2.664	0.8743

Thus the suction reduces the range of lateral variation of the streamlines, and in the limit tends to make them approximately plane curves, when y_b/y_e approaches unity.

Another interesting point shown by the above table is that y_b is always less than y_e, and the streamline near the boundary lags behind the streamline at the edge of the boundary-layer. This result is in agreement with the observation of Rott and Crabtree[17] for zero suction.

(iii) The case $\beta = -1$: $U = U_0 x^{-\frac{1}{3}}$. The projections of all the streamlines on a plane parallel to the wall will be given by

$$\frac{dy}{dx} = \frac{g'}{f'} \tan \gamma \, x^{\frac{1}{3}}.$$

as found by putting $m = -\frac{1}{3}$ in equation (13). The extreme streamlines in plan view are obtained as

$$y_b = \tfrac{3}{4} \frac{g''(0)}{f''(0)} \tan \gamma \, x^{\frac{4}{3}},$$

and .....(19)

$$y_e = \tfrac{3}{4} \tan \gamma \, x^{\frac{4}{3}},$$

the constant of integration being made zero by choosing the origin at $x = 0$ and $y = 0$. Any other intermediate streamline will be given by

$$y = \tfrac{3}{4} \tan \gamma . \, B \, x^{\frac{4}{3}}, \qquad .....(20)$$

where B is an arbitrary constant between $\frac{g''(0)}{f''(0)}$ and unity.

The ratio $\frac{y_b}{y_e}$ then becomes equal to $\frac{g''(0)}{f''(0)}$, and it will be shown below that the ratio decreases with increasing suction and tends to approach unity for very large suctions, but is always greater than unity.

The/

The table is given below:

Table (d)

K	$\frac{y_b}{y_e} = \frac{g''(0)}{f''(0)}$
1.414	∞
1.421	10.786
1.437	6.262
1.50	3.291
1.554	2.640

It is clear from the above results that y_b is always greater than y_e and the streamline nearest the boundary moves ahead of the streamline at the edge of the boundary layer. Also, the suction reduces the lateral spread of the streamlines, and brings them closer to each other in plan view.

5. Secondary Flow in the Boundary Layer

It has been mentioned before that in the presence of a pressure gradient the streamlines in the boundary layer over an infinite yawed cylinder have lateral curvature. This curvature produces a kind of secondary flow in the boundary layer, and it has already been observed by Prandtl[12], Squire[2], Gray[1], Owen and Randall[3], and Stuart[4] as the cause of instability in the boundary layer on a sweptback wing. It has also been found that the velocity profile of this secondary flow, measured in a plane normal to the streamline of the outer flow and normal to the wing surface, has a point of inflexion. The existence of this point of inflexion indicates that above a certain Reynolds number a dynamic instability of the secondary flow may be expected to develop. Powerful vortices will then be formed with their axes nearly parallel to the direction of the outer flow. A Reynolds number for the secondary flow may be defined by

$$\chi = \frac{|v_1|_{max.}\,\delta}{\nu},$$

and the critical value for this number with zero suction has been found, in agreement with wind tunnel and flight observations, to be of the order of 125 by Owen and Randall[3]. The critical value is still to be determined for a porous boundary.

5.1 Secondary flow for 'similar' profiles

If u and v are the velocity components at any point in the chordwise and spanwise directions respectively; and u_1 and v_1 are the components at the same point parallel to and normal to the direction of the edge streamline, then

$$\frac{u_1}{U_1} = f' \cos^2 \theta_e + g' \sin^2 \theta_e$$

and

$$\frac{v_1}{U_1} = \tfrac{1}{2}(g' - f') \sin 2\theta_e \qquad \text{.....(21)}$$

where U_1 = resultant velocity at the edge of the layer and hence $U = U_1 \cos \theta_e$, $V_o = U_1 \sin \theta_e$ and $\theta_e = \tan^{-1}\frac{V_o}{U}$.

The/

The primary flows will be given by the u_1 - profiles and the secondary flows by the v_1 - profiles. These profiles have been obtained for wide ranges of pressure gradients and suctions and have been presented in Tables 7 - 24 and in Figures 1 - 18.

As mentioned before, χ has been taken as a Reynolds number for the secondary flow, and if another Reynolds number for the primary flow is defined as $\chi_1 = \frac{U_1 \delta}{\nu}$, the two Reynolds numbers are related by

$$\frac{\chi}{\chi_1} = \frac{|v_1|_{max}}{U_1} \qquad \ldots\ldots(22)$$

This is the maximum value of $\frac{|v_1|}{U_1}$ and not the value at the point of inflexion of the secondary flow profile. The instability caused by the secondary flow is associated with this ratio of the Reynolds numbers. For practical calculations it will be necessary to find experimentally the maximum value of χ which leads to secondary flow instability in the presence of distributed suction.

This ratio has been plotted against the inclination of the edge streamline (i.e., θ_e) in Fig. 19 for all the cases for which the u_1-and v_1-profiles have been calculated.

6. Discussion of Results

(a) Streamlines. It has been found in (3.0) that the direction of the velocity vector is a function of two parameters θ and ϕ, which depend only on the velocity components u, v and w at the point considered. Also, it has been shown in 4.0 that in the presence of a pressure gradient, the streamlines are curved in three dimensions and reduce to plane curves for zero pressure gradient as in the case of a flat plate. Further, it has been shown that these streamlines can be constructed (e.g., with solid wires) as a three-dimensional model if the direction cosines of the velocity vector are known at every point, in terms of the parameters θ and ϕ. Alternatively the projections of the streamlines on any given plane can be drawn. Thus, the effect of suction on the streamlines can be considered by investigating separately its effects on the streamline projections on the xy and xz planes. The projections on the xy plane, parallel to the boundary, will indicate the lateral curvatures, and the projections on the xz plane, normal to the boundary, will show the normal curvatures of the streamlines.

The most important effect of suction on the streamlines is the reduction of the lateral spread between the two extreme streamlines (on the boundary and at the edge of the boundary layer). The way this effect occurs depends on the pressure gradient. When there is a negative pressure gradient, the value of θ_b increases with suction and, since the value of θ_e remains unaffected, the resultant value of $|\theta_b - \theta_e|$ is greatly reduced, as will be evident from Tables 4 and 6. When there is a positive pressure gradient, the value of θ_b decreases with increasing suction and, since $\theta_b > \theta_e$ the resultant value of $|\theta_b - \theta_e|$ is reduced, as is evident from Tables 5 and 6.

Therefore/

Therefore, since all the other streamlines lie between these two extreme streamlines in plan view, increasing suction brings them closer together until with very large suctions they are approximately plane curves.

There is another important effect of suction on the normal curvature of the streamlines. With increasing suction the value of ϕ increases, (Tables 1, 2 and 3) and the streamlines become more inclined towards the boundary. This effect may occur throughout the boundary layer, or only in a part of the layer near the wall, and at the edge of the boundary layer the streamlines may be directed outwards in the case of very small suctions, as is shown for $K = 0.707$ in Tables 1, 2 and 3.

(b) Combined effect of pressure gradient and suction to produce source or sink-effect

It is found that a strong negative pressure-gradient ($m = +1$) produces a sink-effect (i.e., w negative) throughout the boundary layer, even without suction, as is evident from Table (a) in Section (3.1). For $K = 0$, the suction velocity is zero, but at the edge of the boundary layer the velocity component w is negative and appreciable. When the pressure gradient is zero, not only is the sink-effect absent, but there is a source-effect (i.e., w positive) in the boundary layer, as will be clear from Tables 1, 2 and 3 for $K = 0$, where the value of ϕ are always less than 90^0 throughout the boundary layer. With a positive pressure gradient, the effect is still more pronounced, and for sufficiently large pressure gradients there is a separation of the flow.

Table (a) shows that suction and negative pressure gradient both tend to produce a sink-effect. For regions of constant pressure, even small suctions reduce the source-effect, and moderately large suctions will produce a sink-effect, as shown by Tables 1, 2 and 3. But for positive pressure gradients, the effects of suction become smaller with increasing distance from the boundary, as shown by Table (b). Even a value of K as large as 1.414 is not sufficient to produce a sink-effect at the edge of the boundary layer, whereas for zero pressure gradient this amount of suction does produce a small sink-effect (Tables 1, 2 and 3).

The above discussion of source and sink-effect is of interest, because the source-effect might be expected to lead to instability of the Tollmien-Schlichting type. On this basis, favourable pressure gradients and suction tend to have stabilising effects, and adverse pressure gradients tend to have destabilising effects[13, 14].

(c) Secondary flow (v_1-profiles)

(i) Effect of a pressure gradient

For zero pressure gradient there is no secondary flow in the boundary layer on an infinite yawed cylinder.

A pressure gradient, whether negative or positive, produces a secondary flow which increases with the pressure gradient, as is shown by Tables 7 - 24 and Figs. 1 - 18. Further, it is interesting to note that the secondary flow near the separation point ($\beta = -0.1988$) is more powerful than that near the leading edge ($\beta = 1$), and the two are in opposite directions as can be seen from Tables 7 and 10 and from Figs. 1 and 4, for zero suction.

(ii) Effect of suction

The secondary flow decreases with increasing suction, as shown by Tables 7 to 24 and Figs. 1 - 18. (The v_1-profiles have been given for different suctions, and different pressure gradients for each suction.)

(iii)/

(iii) Variation of the secondary flow with the direction of the edge streamline

Equation (21) shows that the secondary flow is zero when θ_e is $0°$ or $90°$, and that the velocity profiles for this flow are identical at complementary values of θ_e. The maximum secondary flow is obtained when the edge-streamline is inclined at $45°$ to the x-axis, as shown by equation (21), Tables 7 - 24, and Figs. 1 - 18.

(d) u_1-profiles (primary flow)

These profiles have been given in Tables 7 - 24 and Figs. 1 - 18. It can be seen from these tables and figures that the velocity profile u_1/U_1 for any value of θ_c lies between u/U and v/V_o, which are the chordwise and spanwise velocity profiles. When the pressure-gradient is large, the range between these extreme profiles is large, and for a small pressure-gradient the range is very small, as seen from Fig. 6 for $\beta = -0.12$ and $K = 0.2$.

When suction is applied, the range between u/U and v/V_o is reduced and the profiles for different θ_e approach one another as shown by Figs. 1 - 18.

(e) The ratio χ/χ_1 of the Reynolds numbers of the two flows

For any given suction and pressure gradient this ratio

$$\frac{\chi}{\chi_1} = \frac{|v_1|_{max.}\,\delta}{\nu} \Big/ \frac{U_1\,\delta}{\nu}$$

increases with θ_c up to $\theta_c = 45°$, and then decreases again to zero at $\theta_e = 90°$. This variation is shown in Fig. 19, where all the curves are given. It is also clear from Fig. 19 that the pressure gradient increases this ratio, and that suction decreases it, at any value of θ_c except $0°$ and $90°$.

Moreover, Fig. 19 shows that the effect of a positive pressure gradient on the variation of this ratio is more pronounced than that of a negative pressure-gradient. It is interesting here to point out two examples from Fig. 19 to verify the above statement. The first is that for zero suction the curve for $\beta = -0.1988$ is above the curve for $\beta = 1$, even though 1 is much greater than 0.1988. Secondly, the curve for $K = 0$ and $\beta = 1$ is below the curve for $K = 1.554$ and $\beta = -1$, although $|\beta| = 1$ in both cases, and the latter case has a very large suction, whereas the former has zero suction. These results suggest that adverse pressure gradients produce more powerful secondary flows than favourable pressure gradients of the same strength.

7. Conclusions. For a chordwise velocity distribution $U = U_o x^m$.

(1) For zero pressure gradient, the streamlines are plane curves, and have no lateral curvature.

(2) In the presence of a pressure gradient (positive or negative) the streamlines are curved in three dimensions, i.e., they have both lateral and normal curvature.

(3) For negative pressure gradients, the lateral displacement of the wall-streamline lags behind that of the streamline at the edge of the boundary layer, and the reverse is the case for positive pressure gradients.

(4)/

(4) Secondary flow is produced in the boundary-layer due to the lateral curvature of the streamlines.

(5) The secondary flows are opposite in direction for positive and for negative pressure gradients.

(6) The greatest secondary flow is obtained when the edge streamline is inclined at 45° to the chordwise direction.

(7) A pressure gradient whether positive or negative increases the lateral curvature of the streamlines, and thereby the secondary flow, whereas suction reduces the lateral spread of the streamlines and thus decreases the secondary flow.

(8) Suction and negative pressure gradients tend to produce a sink-effect, whereas zero or positive pressure gradients tend to produce a source-effect in the boundary layer.

(9) Secondary flows at complementary angles to the direction of the edge-streamline are equal.

(10) Adverse pressure gradients produce more powerful secondary flows than favourable pressure gradients of the same numerical strength.

8. Acknowledgements

I wish to acknowledge the financial help given by the Government of India and the Patna University in the form of a scholarship for my work at Cambridge. I am very grateful to Dr. J. H. Preston, who supervised the work; and to Professor W. A. Mair, Dr. M. R. Head and Dr. B. G. Newman for their sympathetic interest in the problem.

References

No.	Author(s)	Title, etc.
1	Gray, W. E.	A laminar flow experiment in flight on a swept wing. R.A.E. Tech. Note Aero. 2240. A.R.C.16,032. March, 1953.
2	Squire, H. B.	Addendum to: A.R.C.15,022 Boundary-layer transition on a sweptback wing, by P. R. Owen and D. G. Randall. R.A.E. Tech. Memo. No. Aero 277, May, 1952 . June, 1952.
3	Owen, P. R. and Randall, D. G.	Boundary-layer transition on a sweptback wing: a further investigation. R.A.E. Tech. Memo. No. Aero. 330. A.R.C.15,741. February, 1953.
4	Stuart, J. T.	An interim note on the stability of the boundary-layer on a swept wing. A.R.C.14,991. June, 1952.
5	Gray, W. E.	The effect of wing sweep on laminar flow. R.A.E. Tech. Memo. No. Aero.255, A.R.C.14,929. February, 1952.

6./

No.	Author(s)	Title, etc.
6	Owen, P. R. and Randall, D. G.	The use of distributed suction to delay boundary-layer transition on a sweptback wing. R.A.E. Tech. Memo. No. Aero.353. A.R.C.15,798. March, 1953.
7	Hartree, D. R.	On an equation occurring in Falkner and Skan's approximate treatment of the equations of the boundary-layer. Proc. Camb. Phil. Soc., Vol. 33 (1937), pp.223 - 239.
8	Cooke, J. C.	The boundary-layer of a class of infinite cylinders. Proc. Camb. Phil. Soc., Vol. 46, Part 4, October, 1950, p.645.
9	Schlichting, H. and Bussmann, K.	Exakte Lösungen für die Laminare Grenzschicht mit Absagung und Ausblasen. Sonderdruck aus Band 7 B, (1943) Heft 2, der Deutschen Akademie der wuftfahrtforschung.
10	Thwaites, B.	The development of laminar boundary-layers under conditions of continuous suction. Part II. Approximate methods of solution. A.R.C.12,699. 8th November, 1949.
11	Sinha, K. D. P.	The laminar boundary-layer with distributed suction on an infinite yawed cylinder. C.P. 214. November, 1954.
12	Prandtl, L.	On boundary-layers in three-dimensional flow. M.A.P. Völkenrode, M.A.P. - VG 84 - 64 T, May, 1946.
13	Schlichting, H.	Boundary-layer theory. Pergamon Press 1955.
14	Tollmien, W, Ulrich, A, Pretsch, J. and Schlichting, H.	A.V.A. Monographs, Reports and Translations No.1001, 1004 and 1005. (1948)
15	Sears, W. R.	The boundary-layer of yawed cylinders. Journal of Aeronautical Sciences, Vol. 15, No. 1, January, 1948.
16	Wild, J. M.	The boundary-layer on infinite yawed cylinders: Journal of the Aeronautical Sciences, Vol. 16, No. 1, 1949.
17	Rott, N. and Crabtree, L. F.	Simplified laminar boundary-layer calculations for bodies of revolution and for yawed wings. Journal of Aeronautical Sciences, Vol. 19, No. 8, August, 1952.

TABLE 1/

TABLE 1

Results of the calculation of ϕ for the flat plate

γ (sweep) = 15°

(a) K = 0

$R_x \rightarrow$	10	10^3	10^4	2×10^5
η	ϕ	ϕ	ϕ	ϕ
0	90°	90°	90°	90°
1	85°39'	88°37'	89°52'	89°58'
3	78°22'	86°16'	89°38'	89°55'
5.0	75°32'	85°20'	89°32'	89°54'
7.8	75°17'	85°15'	89°31'	89°54'

(b) K = 0.7070

$R_x \rightarrow$	10	10^3	10^4	2×10^5	10^7	6×10^7
η	ϕ	ϕ	ϕ	ϕ	ϕ	ϕ
0	180°	180°	180°	180°	180°	180°
1	101°20'	90°38'	90°22'	90°5'	90°	90°
2	93°17'	91°2'	90°6'	90°2'	90°	90°
3	90°32'	90°10'	90°1'	90°	90°	90°
3.4	90°12'	90°4'	90°	90°	90°	90°
3.6	89°57'	90°	90°	90°	90°	90°
4.4	89°38'	89°53'	90°	90°	90°	90°

(c) K = 1.414

$R_x \rightarrow$	10^3	10^4	2×10^5	6×10^7	5×10^6
η	ϕ	ϕ	ϕ	ϕ	ϕ
0	180°	180°	180°	180°	180°
1	96°24'	90°39'	90°9'	90°	90°
2	94°3'	90°24'	90°3'	90°	90°
3	93°35'	90°21'	90°5'	90°	90°
3.4	93°31'	90°21'	90°5'	90°	90°

(d)/

TABLE 1 (cont.)

(d) K = 3.535

$R_x \rightarrow$	10^2	10^4	2×10^5	5×10^8	10^{10}
η	ϕ	ϕ	ϕ	ϕ	ϕ
0	180°	180°	180°	180°	180°
0.2	120°31'	93°23'	90°45'	90°	90°
0.8	104°34'	91°29'	90°20'	90°	90°
2.0	102°42'	91°17'	90°17'	90°	90°
2.4	102°36'	91°17'	90°17'	90°	90°

(e) K = 7.070

$R_x \rightarrow$	10^2	10^4	2×10^5	10^{10}	2×10^{11}
η	ϕ	ϕ	ϕ	ϕ	ϕ
0	180°	180°	180°	180°	180°
0.1	140°30'	96°55'	91°33'	90°	90°
0.4	118°45'	93°8'	90°42'	90°	90°
1.0	115°28'	92°43'	90°37'	90°	90°
1.2	115°21'	92°43'	90°36'	90°	90°

(f) K = 14.14

$R_x \rightarrow$	10	10^2	10^4	2×10^5	10^{10}	2×10^{11}
η	ϕ	ϕ	ϕ	ϕ	ϕ	ϕ
0	180°	180°	180°	180°	180°	180°
0.1	168°14'	146°39'	90°38'	91°57'	90°	90°
0.2	164°9'	138°4'	96°21'	91°26'	90°	90°
0.4	162°8'	134°27'	95°36'	91°15'	90°	90°
0.8	161°47'	133°52'	95°29'	91°14'	90°	90°

TABLE 2/

TABLE 2

Results of the calculation of ϕ for the flat plate

γ (sweep) = 45°

(a) K = 0

$R_x \rightarrow$	10	10^3	10^4	2×10^5
η	ϕ	ϕ	ϕ	ϕ
0	90°	90°	90°	90°
1	86°49'	88°53'	89°54'	89°58'
3	81°26'	87°16'	89°44'	89°56'
5	79°18'	86°35'	89°40'	89°55'
7.8	79°6'	86°31'	89°39'	89°55'

(b) K = 0.7070

$R_x \rightarrow$	10	10^3	10^4	2×10^5	10^7	6×10^7
η	ϕ	ϕ	ϕ	ϕ	ϕ	ϕ
0	180°	180°	180°	180°	180°	180°
1	98°21'	92°39'	90°16'	90°4'	90°	90°
2	92°24'	90°46'	90°5'	90°1'	90°	90°
3	90°24'	90°7'	90°	90°	90°	90°
3.4	90°9'	90°3'	90°	90°	90°	90°
3.6	89°58'	90°	90°	90°	90°	90°
4.4	89°44'	89°55'	90°	90°	90°	90°

(c) K = 1.414

$R_x \rightarrow$	10^3	10^4	2×10^5	6×10^7	5×10^8
η	ϕ	ϕ	ϕ	ϕ	ϕ
0	180°	180°	180°	180°	180°
1	91°42'	90°28'	90°6'	90°	90°
2	92°58'	90°18'	90°4'	90°	90°
3	92°37'	90°16'	90°3'	90°	90°
3.4	92°34'	90°15'	90°3'	90°	90°

(a)/

TABLE 2 (cont.)

(d) K = 3.535

$R_x \rightarrow$	10^2	10^4	2×10^5	5×10^8	10^{10}
η	ϕ	ϕ	ϕ	ϕ	ϕ
0	180°	180°	180°	180°	180°
0.2	113°21'	92°28'	90°33'	90°	90°
0.8	100°47'	91°5'	90°15'	90°	90°
2.0	99°22'	90°57'	90°13'	90°	90°
2.4	99°18'	90°56'	90°13'	90°	90°

(e) K = 7.070

$R_x \rightarrow$	10^2	10^4	2×10^5	10^{10}	2×10^{11}
η	ϕ	ϕ	ϕ	ϕ	ϕ
0	180°	180°	180°	180°	180°
0.1	131°36'	95°4'	91°8'	90°	90°
0.4	111°53'	92°18'	90°31'	90°	90°
1.0	109°13'	92°	90°27'	90°	90°
1.2	109°7'	91°59'	90°27'	90°	90°

(f) K = 14.14

$R_x \rightarrow$	10	10^2	10^4	2×10^5	10^{10}	2×10^{11}
η	ϕ	ϕ	ϕ	ϕ	ϕ	ϕ
0	180°	180°	180°	180°	180°	180°
0.1	164°9'	138°9'	96°56'	91°25'	90°	90°
0.2	158°47'	129°11'	94°39'	91°3'	90°	90°
0.4	156°15'	125°41'	94°7'	90°55'	90°	90°
0.8	155°48'	125°8'	94°1'	90°54'	90°	90°

TABLE 3/

TABLE 3

Results of the calculation of ϕ for the flat plate

γ (sweep) = 60°

(a) K = 0

$R_x \rightarrow$	10	10^3	10^4	2×10^5
η	ϕ	ϕ	ϕ	ϕ
0	90°	90°	90°	90°
1	87°45'	89°17'	89°56'	89°59'
3	83°55'	83°4'	89°48'	89°57'
5	82°24'	87°35'	89°45'	89°57'
7.8	82°15'	87°32'	89°45'	89°57'

(b) K = 0.7070

$R_x \rightarrow$	10	10^3	10^4	2×10^5	10^7	6×10^7
η	ϕ	ϕ	ϕ	ϕ	ϕ	ϕ
0	180°	180°	180°	180°	180°	180°
1	95°55'	91°53'	9[illegible]°11'	90°3'	90°	90°
2	91°42'	90°32'	90°3'	90°1'	90°	90°
3	90°17'	90°5'	90°	90°	90°	90°
3.4	90°6'	90°2'	90°	90°	90°	90°
3.6	89°59'	90°	90°	90°	90°	90°
4.4	89°48'	89°56'	90°	90°	90°	90°

(c) K = 1.414

$R_x \rightarrow$	10^3	10^4	2×10^6	6×10^7	5×10^8
η	ϕ	ϕ	ϕ	ϕ	ϕ
0	180°	180°	180°	180°	180°
1	93°20'	90°20'	90°5'	90°	90°
2	92°6'	90°13'	90°3'	90°	90°
3	91°51'	90°11'	90°3'	90°	90°
3.4	91°49'	90°11'	90°3'	90°	90°

(d)

TABLE 3 (cont.)

(d) K = 3.535

$R_x \rightarrow$	10^2	10^4	2×10^5	5×10^8	10^{10}
η	ϕ	ϕ	ϕ	ϕ	ϕ
0	180°	180°	180°	180°	180°
0.2	106°58'	91°45'	90°23'	90°	90°
0.8	97°39'	90°46'	90°10'	90°	90°
2.0	96°39'	90°40'	90°9'	90°	90°
2.4	96°36'	90°40'	90°9'	90°	90°

(e) K = 7.070

$R_x \rightarrow$	10^2	10^4	2×10^5	10^{10}	2×10^{11}
η	ϕ	ϕ	ϕ	ϕ	ϕ
0	180°	180°	180°	180°	180°
0.1	122°7'	93°36'	90°48'	90°	90°
0.4	105°51'	91°38'	90°23'	90°	90°
1.0	103°51'	91°25'	90°19'	90°	90°
1.2	103°46'	91°24'	90°19'	90°	90°

(f) K = 14.14

$R_x \rightarrow$	10	10^2	10^4	2×10^5	10^{10}	2×10^{11}
η	ϕ	ϕ	ϕ	ϕ	ϕ	ϕ
0	180°	180°	180°	180°	180°	180°
0.1	158°6'	128°11'	94°30'	91°	90°	90°
0.2	151°15'	119°57'	93°18'	90°44'	90°	90°
0.4	148°6'	116°56'	92°54'	90°39'	90°	90°
0.8	147°34'	116°28'	92°51'	90°38'	90°	90°

TABLE 4/

TABLE 4

Results of the calculation of θ for the stagnation flow

(a) $K = 0$, $\beta = 1$

$\theta_e \rightarrow$ / $\eta \downarrow$	90° θ	75° θ	45° θ	15° θ	0° θ
0	90°	59°56'	24°50'	7°4'	0°
0.4	90°	63°59'	28°46'	8°22'	0°
0.8	90°	67°37'	33°3'	9°53'	0°
1.2	90°	70°27'	37°2'	11°26'	0°
1.6	90°	72°26'	40°15'	12°47'	0°
2.0	90°	73°42'	42°30'	13°47'	0°
2.4	90°	74°24.5'	43°50'	14°26'	0°
2.8	90°	74°46'	44°32'	14°46'	0°
3.2	90°	74°55'	44°50'	14°55'	0°
3.6	90°	74°58.5'	44°57'	14°59'	0°
4.0	90°	74°59'	44°59'	15°	0°
4.3	90°	75°	45°	15°	0°

(b) $K = 0.5$, $\beta = 1$

$\theta_e \rightarrow$ / $\eta \downarrow$	90° θ	75° θ	45° θ	15° θ	0° θ
0	90°	65°53'	30°54'	9°6'	0°
0.4	90°	68°39'	34°26'	10°25'	0°
0.8	90°	71°3'	38°58'	11°49'	0°
1.2	90°	72°48'	40°53'	13°3'	0°
1.6	90°	73°54'	42°53'	13°58'	0°
2.0	90°	74°32'	44°4'	14°32'	0°
2.4	90°	74°50'	44°39'	14°50'	0°
2.8	90°	74°57'	44°54'	14°57'	0°
3.2	90°	74°59'	44°59'	15°	0°
3.3	90°	75°	45°	15°	0°

(c)/

TABLE 4 (cont.)

(c) K = 2.664, β = 1

$\theta_e \rightarrow$ η	90° θ	75° θ	45° θ	15° θ	0° θ
0	90°	72°58'	41°10'	13°11'	0
0.326	90°	73°51'	42°46'	13°55'	0
0.726	90°	74°32'	44°4'	14°33'	0
1.126	90°	74°51'	44°42'	14°51'	0
1.526	90°	74°58'	44°55'	14°58'	0
1.926	90°	74°59'	44°59'	15°	0
2.326	90°	75°	45°	15°	0

TABLE 5

Results of the calculation of θ for the case $U = U_o x^{-\frac{1}{3}}$

(a) K = 1.414, β = -1

$\theta_e \rightarrow$ Y	0° θ	15° θ	45° θ	75° θ	90° θ
0	0°	90°	90°	90°	90°
0.5	0°	55°20'	79°30'	87°9'	90°
1.0	0°	33°39'	68°4'	83°51'	90°
1.5	0°	23°14'	58°2'	80°30'	90°
2.0	0°	18°22'	51°6'	77°48'	90°
2.5	0°	16°11'	47°17.5'	76°6'	90°
3.0	0°	15°21'	45°41'	75°20'	90°
3.5	0°	15°5'	45°10'	75°5'	90°
4.0	0°	15°1'	45°2'	75°1'	90°
4.25	0°	15°	45°	75°	90°

(b)/

TABLE 5 (cont.)

(b) K = 1.554, β = -1

$\theta_e \rightarrow$ Y $\downarrow$	0° θ	15° θ	45° θ	75° θ	90° θ
0	0°	35°17'	69°15'	84°12'	90°
0.5	0°	26°23.5'	61°38'	81°46'	90°
1.0	0°	20°35'	54°30'	79°11'	90°
1.5	0°	18°23'	49°25.5'	77°5'	90°
2.0	0°	15°50'	46°37'	75°48'	90°
2.5	0°	15°14'	45°27'	75°13.5'	90°
3.0	0°	15°3'	45°6'	75°3'	90°
3.5	0°	15°1'	45°2'	75°1'	90°
4.0	0°	15°	45°	75°	90°

TABLE 6

Results of the calculation of the differences of the two extreme values of θ (on the boundary and the edge of the boundary-layer).

	$\theta_e \rightarrow$	0°	15°	45°	75°	90°
K	β	$\lvert\theta_e-\theta_b\rvert$	$\lvert\theta_e-\theta_b\rvert$	$\lvert\theta_e-\theta_b\rvert$	$\lvert\theta_e-\theta_b\rvert$	$\lvert\theta_e-\theta_b\rvert$
0	1	0°	7°56'	20°10'	15°4'	0°
0.5	1	0°	5°54'	14°6'	9°7'	0°
2.664	1	0°	1°49'	3°50'	2°2'	0°
1.414	-1	0°	75°	45°	15°	0°
1.554	-1	0°	20°17'	24°15'	9°12'	0°

TABLE 7/

TABLE 7

Primary and secondary flow profiles for the stagnation flow and zero suction

K = 0, β = 1

$\theta_e \rightarrow$	90°	75°	60°	45°	30°	15°	0°	75°,15°	30°,60°	45°
η	$\frac{u_1}{U_1}=\frac{\vartheta}{V_o}$	$\frac{u_1}{U_1}$	$\frac{u_1}{U_1}$	$\frac{u_1}{U_1}$	$\frac{u_1}{U_1}$	$\frac{u_1}{U_1}$	$\frac{u_1}{U_1}=\frac{u}{U}$	$\frac{\vartheta_1}{U_1}$	$\frac{\vartheta_1}{U_1}$	$\frac{\vartheta_1}{U_1}$
0		0	0	0	0	0		0	0	0
0.1		0.0611	0.0723	0.0876	0.1030	0.1142		-0.0153	-0.0265	-0.0306
0.2		0.1215	0.1421	0.1703	0.1984	0.2191		-0.0281	-0.0487	-0.0563
0.3		0.1812	0.2095	0.2480	0.2866	0.3149		-0.0386	-0.0668	-0.0771
0.4		0.2400	0.2742	0.3209	0.3677	0.4019		-0.0467	-0.0809	-0.0934
0.5		0.2976	0.3363	0.3890	0.4418	0.4805		-0.0528	-0.0914	-0.1055
0.6		0.3540	0.3956	0.4525	0.5093	0.5510		-0.0568	-0.0985	-0.1137
0.7		0.4080	0.4515	0.5109	0.5704	0.6139		-0.0594	-0.1029	-0.1188
0.8		0.4622	0.5060	0.5660	0.6259	0.6698		-0.0599	-0.1038	-0.1199
0.9		0.5133	0.5568	0.6162	0.6756	0.7191		-0.0594	-0.1029	-0.1188
1.0	Reference (11)	0.5623	0.6045	0.6623	0.7200	0.7623	Reference (9)	-0.0577	-0.1000	-0.1155
1.2		0.6526	0.6907	0.7427	0.7947	0.8328		-0.0520	-0.0901	-0.1040
1.4		0.7317	0.7641	0.8083	0.8526	0.8849		-0.0442	-0.0766	-0.0884
1.6		0.7987	0.8249	0.8607	0.8966	0.9228		-0.0358	-0.0620	-0.0716
1.8		0.8535	0.8738	0.9015	0.9292	0.9495		-0.0277	-0.0480	-0.0554
2.0		0.8967	0.9117	0.9322	0.9527	0.9677		-0.0205	-0.0355	-0.0410
2.2		0.9295	0.9402	0.9548	0.9695	0.9802		-0.0146	-0.0253	-0.0292
2.4		0.9535	0.9607	0.9706	0.9806	0.9878		-0.0099	-0.0172	-0.0198
2.6		0.9702	0.9750	0.9815	0.9881	0.9928		-0.0065	-0.0113	-0.0130
2.8		0.9817	0.9847	0.9888	0.9930	0.9960		-0.0041	-0.0071	-0.0082
3.0		0.9891	0.9909	0.9934	0.9960	0.9978		-0.0025	-0.0044	-0.0050
3.2		0.9937	0.9948	0.9962	0.9977	0.9988		-0.0015	-0.0025	-0.0029
3.4		0.9965	0.9971	0.9979	0.9988	0.9994		-0.0008	-0.0014	-0.0016
3.6		0.9982	0.9985	0.9989	0.9994	0.9997		-0.0004	-0.0007	-0.0008
3.8		0.9991	0.9992	0.9994	0.9997	0.9998		-0.0002	-0.0004	-0.0004
4.0		0.9995	0.9996	0.9997	0.9999	1.0		-0.0001	-0.0002	-0.0002
4.2		0.9998	0.9998	0.9999	0.9999	1.0		-0.00005	-0.0001	-0.0001
4.4		0.9999	0.9999	0.9999	1.0	1.0		-0.00002	-0.00004	-0.00005
		1.0	1.0	1.0	1.0	1.0		0	0	0

Note: ϑ_1 is zero for θ_e = 0° and 90°.

TABLE 8/

TABLE 8

Primary and secondary flow profiles for the stagnation flow with suction

$K = 0.5, \beta = 1$

$\theta_e \rightarrow$	90°	75°	60°	45°	30°	15°	0°	15°,75°	30°,60°	45°
η	$\frac{u_1}{U_1}=\frac{\vartheta}{V_o}$	$\frac{u_1}{U_1}$	$\frac{u_1}{U_1}$	$\frac{u_1}{U_1}$	$\frac{u_1}{U_1}$	$\frac{u_1}{U_1}$	$\frac{u_1}{U_1}=\frac{u}{U}$	$\frac{\vartheta_1}{U_1}$	$\frac{\vartheta_1}{U_1}$	$\frac{\vartheta_1}{U_1}$
0		0	0	0	0	0		0	0	0
0.1		0.0937	0.1039	0.1177	0.1316	0.1418		-0.0139	-0.0240	-0.0277
0.2		0.1821	0.2002	0.2248	0.2495	0.2676		-0.0247	-0.0427	-0.0493
0.3		0.2654	0.2893	0.3220	0.3547	0.3786		-0.0327	-0.0566	-0.0654
0.4		0.3435	0.3715	0.4097	0.4479	0.4759		-0.0382	-0.0662	-0.0764
0.5		0.4166	0.4470	0.4885	0.5301	0.5605		-0.0415	-0.0719	-0.0830
0.6		0.4846	0.5161	0.5591	0.6021	0.6336		-0.0430	-0.0745	-0.0860
0.7		0.5475	0.5789	0.6219	0.6649	0.6964		-0.0430	-0.0744	-0.0859
0.8		0.6053	0.6359	0.6776	0.7194	0.7500		-0.0418	-0.0723	-0.0835
0.9		0.6580	0.6870	0.7267	0.7663	0.7954		-0.0396	-0.0687	-0.0793
1.0		0.7059	0.7329	0.7697	0.8066	0.8336		-0.0369	-0.0639	-0.0737
1.1		0.7488	0.7735	0.8072	0.8409	0.8656		-0.0337	-0.0584	-0.0674
1.2	Reference (11)	0.7872	0.8094	0.8396	0.8699	0.8921	Reference (9)	-0.0303	-0.0524	-0.0605
1.3		0.8211	0.8407	0.8675	0.8944	0.9140		-0.0268	-0.0465	-0.0536
1.4		0.8508	0.8679	0.8913	0.9148	0.9319		-0.0234	-0.0406	-0.0468
1.5		0.8766	0.8914	0.9115	0.9317	0.9465		-0.0202	-0.0349	-0.0403
1.6		0.8988	0.9113	0.9285	0.9456	0.9582		-0.0171	-0.0297	-0.0343
1.7		0.9178	0.9283	0.9427	0.9571	0.9676		-0.0144	-0.0249	-0.0288
1.8		0.9337	0.9424	0.9544	0.9663	0.9751		-0.0119	-0.0207	-0.0239
1.9		0.9471	0.9543	0.9641	0.9739	0.9811		-0.0098	-0.0170	-0.0196
2.0		0.9582	0.9640	0.9719	0.9799	0.9857		-0.0079	-0.0137	-0.0158
2.1		0.9673	0.9719	0.9783	0.9846	0.9893		-0.0063	-0.0110	-0.0127
2.2		0.9746	0.9783	0.9833	0.9884	0.9920		-0.0050	-0.0087	-0.0100
2.3		0.9806	0.9835	0.9874	0.9913	0.9941		-0.0039	-0.0067	-0.0078
2.4		0.9854	0.9876	0.9905	0.9935	0.9957		-0.0030	-0.0051	-0.0059
2.5		0.9891	0.9908	0.9930	0.9953	0.9970		-0.0023	-0.0039	-0.0045
2.6		0.9920	0.9933	0.9949	0.9966	0.9978		-0.0017	-0.0029	-0.0033
2.7		0.9943	0.9952	0.9964	0.9977	0.9986		-0.0012	-0.0021	-0.0024
2.8		0.9960	0.9967	0.9975	0.9984	0.9991		-0.0009	-0.0015	-0.0017
2.9		0.9974	0.9978	0.9984	0.9990	0.9994		-0.0006	-0.0010	-0.0012
3.0		0.9983	0.9986	0.9990	0.9994	0.9997		-0.0004	-0.0007	-0.0008
3.1		0.9991	0.9992	0.9994	0.9997	0.9998		-0.0002	-0.0004	-0.0004
3.2		0.9996	0.9997	0.9998	0.9999	1.0		-0.0001	-0.0002	-0.0002
3.3		1.0	1.0	1.0	1.0	1.0		- 0	- 0	- 0

Note: ϑ_1 is zero for $\theta_e = 0°$ and $90°$.

TABLE 9/

TABLE 9

Primary and secondary flow profiles for the stagnation flow with suction

$K = 2.664, \quad \beta = 1$

$\theta_e \rightarrow$	90°	75°	60°	45°	30°	15°	0°	15°,75°	30°,60°	45°
η	$\frac{u_1}{U_1}=\frac{\vartheta}{V_o}$	$\frac{u_1}{U_1}$	$\frac{u_1}{U_1}$	$\frac{u_1}{U_1}$	$\frac{u_1}{U_1}$	$\frac{u_1}{U_1}$	$\frac{u_1}{U_1}=\frac{u}{U}$	$\frac{\vartheta_1}{U_1}$	$\frac{\vartheta_1}{U_1}$	$\frac{\vartheta_1}{U_1}$
0		0	0	0	0	0		0	0	0
0.026		0.0715	0.0727	0.0742	0.0758	0.0770		-0.0016	-0.0027	-0.0031
0.126		0.3053	0.3114	0.3197	0.3281	0.3342		-0.0083	-0.0144	-0.0166
0.226		0.4835	0.4920	0.5035	0.5151	0.5236		-0.0116	-0.0200	-0.0231
0.326		0.6187	0.6278	0.6403	0.6527	0.6619		-0.0124	-0.0216	-0.0249
0.426		0.7207	0.7294	0.6963	0.7533	0.7620		-0.0119	-0.0206	-0.0238
0.526		0.7970	0.8048	0.8154	0.8261	0.8338		-0.0106	-0.0184	-0.0212
0.626		0.8537	0.8603	0.8695	0.8784	0.8850		-0.0090	-0.0156	-0.0180
0.726		0.8956	0.9009	0.9083	0.9156	0.9210		-0.0073	-0.0127	-0.0147
0.826	Reference (11)	0.9261	0.9305	0.9361	0.9420	0.9462	Reference (9)	-0.0058	-0.0101	-0.0116
0.926		0.9481	0.9514	0.9559	0.9604	0.9637		-0.0045	-0.0078	-0.0090
1.026		0.9639	0.9664	0.9698	0.9732	0.9757		-0.0034	-0.0059	-0.0068
1.126		0.9752	0.9770	0.9795	0.9820	0.9838		-0.0025	-0.0043	-0.0050
1.226		0.9832	0.9845	0.9863	0.9881	0.9894		-0.0018	-0.0031	-0.0036
1.326		0.9886	0.9896	0.9908	0.9921	0.9930		-0.0013	-0.0022	-0.0025
1.426		0.9924	0.9931	0.9940	0.9949	0.9955		-0.0009	-0.0015	-0.0018
1.526		0.9950	0.9954	0.9960	0.9967	0.9971		-0.0006	-0.0011	-0.0012
1.626		0.9967	0.9970	0.9974	0.9979	0.9982		-0.0004	-0.0007	-0.0008
1.726		0.9980	0.9982	0.9984	0.9987	0.9989		-0.0003	-0.0005	-0.0005
1.826		0.9989	0.9990	0.9991	0.9993	0.9994		-0.0001	-0.0002	-0.0002
1.926		0.9992	0.9993	0.9994	0.9995	0.9996		-0.00010	-0.0002	-0.0002
2.026		0.9995	0.9996	0.9996	0.9997	0.9998		-0.00007	-0.00010	-0.00015
2.126		0.9997	0.9997	0.9998	0.9998	0.9999		-0.00005	-0.00009	-0.00010
2.226		0.9999	0.9999	0.9999	1.0	1.0		-0.00002	-0.00004	-0.00005
2.326		1.0	1.0	1.0	1.0	1.0		0	0	0

Note: ϑ_1 is zero for $\theta_e = 0°$ and $90°$.

TABLE 10/

TABLE 10

Primary and secondary flow profiles for the separation case with zero suction

K = 0, β = - 0.1988

$\theta_e \rightarrow$	0°	15°	30°	45°	60°	75°	90°	15°,75°	30°,60°	45°
Y	$\frac{u_1}{U_1}=\frac{u}{U}$	$\frac{u_1}{U_1}$	$\frac{u_1}{U_1}$	$\frac{u_1}{U_1}$	$\frac{u_1}{U_1}$	$\frac{u_1}{U_1}$	$\frac{u_1}{U_1}=\frac{\vartheta}{V_o}$	$\frac{\vartheta_1}{U_1}$	$\frac{\vartheta_1}{U_1}$	$\frac{\vartheta_1}{U_1}$
0		0	0	0	0	0		0	0	0
0.4		0.0237	0.0446	0.0731	0.0981	0.1226		0.0286	0.0495	0.0571
0.8		0.0772	0.1131	0.1622	0.2114	0.2473		0.0491	0.0851	0.0982
1.2		0.1586	0.2039	0.2658	0.3277	0.3730		0.0619	0.1072	0.1238
1.6		0.2678	0.3164	0.3828	0.4493	0.4949		0.0664	0.1150	0.1328
2.0	Reference (7)	0.3971	0.4437	0.5075	0.5712	0.6179	Reference (8)	0.0637	0.1104	0.1275
2.4		0.5377	0.5778	0.6327	0.6875	0.7277		0.0548	0.0950	0.1097
2.8		0.6753	0.7061	0.7482	0.7903	0.8211		0.0421	0.0729	0.0842
3.2		0.7937	0.8147	0.8435	0.8722	0.8933		0.0287	0.0498	0.0575
3.6		0.8836	0.8962	0.9133	0.9305	0.9431		0.0172	0.0297	0.0343
4.0		0.9424	0.9489	0.9578	0.9667	0.9732		0.0089	0.0154	0.0178
4.4		0.9751	0.9780	0.9820	0.9860	0.9889		0.0040	0.0069	0.0080
4.8		0.9904	0.9916	0.9932	0.9949	0.9961		0.0016	0.0028	0.0032
5.2		0.9971	0.9975	0.9979	0.9984	0.9988		0.0005	0.0008	0.0009
5.6		0.9990	0.9992	0.9993	0.9995	0.9996		0.0002	0.0003	0.0003
6.0		1.0	1.0	0.9999	0.9999	0.9999		0	0	0
6.4		1.0	1.0	1.0	1.0	1.0		0	0	0

Note: ϑ_1 is zero for θ_e = 0° and 90°

TABLE 11

Primary and secondary flow profiles with a positive pressure gradient and suction (separation case).

K = 0.2, β = - 0.28

$\theta_e \rightarrow$	0°	15°	30°	45°	60°	75°	90°	15°,75°	30°,60°	45°
Y	$\frac{u_1}{U_1}=\frac{u}{U}$	$\frac{u_1}{U_1}$	$\frac{u_1}{U_1}$	$\frac{u_1}{U_1}$	$\frac{u_1}{U_1}$	$\frac{u_1}{U_1}$	$\frac{u_1}{U_1}=\frac{\vartheta}{V_o}$	$\frac{\vartheta_1}{U_1}$	$\frac{\vartheta_1}{U_1}$	$\frac{\vartheta_1}{U_1}$
0		0	0	0	0	0		0	0	0
0.5		0.0474	0.0815	0.1280	0.1745	0.2085		0.0465	0.0805	0.0930
1.0		0.1522	0.2048	0.2765	0.3483	0.4001		0.0718	0.1243	0.1435
1.5		0.3049	0.3619	0.4398	0.5178	0.5748		0.0779	0.1350	0.1558
2.0	Reference (10)	0.4873	0.5375	0.6059	0.6744	0.7245	Reference (11)	0.0685	0.1186	0.1369
2.5		0.6694	0.7058	0.7557	0.8055	0.8420		0.0498	0.0863	0.0997
3.0		0.8199	0.8416	0.8711	0.9007	0.9224		0.0296	0.0512	0.0591
3.5		0.9197	0.9300	0.9440	0.9580	0.9682		0.0140	0.0242	0.0280
4.0		0.9714	0.9752	0.9805	0.9857	0.9896		0.0052	0.0091	0.0105
4.5		0.9924	0.9934	0.9948	0.9963	0.9973		0.0014	0.0025	0.0028
5.0		0.9990	0.9991	0.9993	0.9994	0.9996		0.0001	0.0003	0.0003
5.5		1.0	1.0	1.0	1.0	1.0		0	0	0

Note: ϑ_1 is zero for θ_e = 0° and 90°.

TABLE 12/

TABLE 12

Primary and secondary flow profiles with a positive pressure gradient and suction

K = 0.2, β = - 0.12

$\theta_e \rightarrow$	0°	15°	30°	45°	60°	75°	90°	15°,75°	30°,60°	45°
Y	$\frac{u_1}{U_1}=\frac{u}{U}$	$\frac{u_1}{U_1}$	$\frac{u_1}{U_1}$	$\frac{u_1}{U_1}$	$\frac{u_1}{U_1}$	$\frac{u_1}{U_1}$	$\frac{u_1}{U_1}=\frac{\vartheta}{V_o}$	$\frac{\vartheta_1}{U_1}$	$\frac{\vartheta_1}{U_1}$	$\frac{\vartheta_1}{U_1}$
0		0	0	0	0	0		0	0	0
0.5		0.2352	0.2441	0.2562	0.2684	0.2772		0.0121	0.0210	0.0242
1.0		0.4653	0.4772	0.4934	0.5096	0.5215		0.0162	0.0281	0.0324
1.5	Reference (10)	0.6707	0.6810	0.6950	0.7090	0.7192	Reference (11)	0.0140	0.0243	0.0280
2.0		0.8274	0.8341	0.8432	0.8523	0.8590		0.0091	0.0158	0.0182
2.5		0.9252	0.9285	0.9331	0.9376	0.9410		0.0045	0.0079	0.0091
3.0		0.9735	0.9748	0.9766	0.9785	0.9798		0.0018	0.0032	0.0036
3.5		0.9931	0.9934	0.9938	0.9942	0.9945		0.0004	0.0007	0.0008
4.0		0.9990	0.9989	0.9988	0.9988	0.9987		0	0	0
4.5		1.0	0.9999	0.9998	0.9997	0.9996		0	0	0
5.0		1.0	0.9999	0.9999	0.9998	0.9998		0	0	0
5.5		1.0	1.0	1.0	1.0	1.0		0	0	0

Note: ϑ_1 is zero for θ_e = 0° and 90°.

TABLE 13

Primary and secondary flow profiles with a positive pressure gradient and suction (separation case).

K = 0.4, β = - 0.371

$\theta_e \rightarrow$	0°	15°	30°	45°	60°	75°	90°	15°,75°	30°,60°	45°
Y	$\frac{u_1}{U_1}=\frac{u}{U}$	$\frac{u_1}{U_1}$	$\frac{u_1}{U_1}$	$\frac{u_1}{U_1}$	$\frac{u_1}{U_1}$	$\frac{u_1}{U_1}$	$\frac{u_1}{U_1}=\frac{\vartheta}{V_o}$	$\frac{\vartheta_1}{U_1}$	$\frac{\vartheta_1}{U_1}$	$\frac{\vartheta_1}{U_1}$
0		0	0	0	0	0		0	0	0
0.5		0.0597	0.1026	0.1612	0.2198	0.2627		0.0586	0.1015	0.1172
1.0		0.1850	0.2478	0.3335	0.4193	0.4821		0.0858	0.1486	0.1715
1.5	Reference (10)	0.3594	0.4233	0.5105	0.5978	0.6617	Reference (11)	0.0873	0.1512	0.1745
2.0		0.5550	0.6069	0.6777	0.7486	0.8005		0.0709	0.1227	0.1417
2.5		0.7364	0.7705	0.8169	0.8634	0.8974		0.0462	0.0801	0.0924
3.0		0.8715	0.8893	0.9135	0.9378	0.9556		0.0243	0.0420	0.0485
3.5		0.9487	0.9562	0.9665	0.9767	0.9842		0.0102	0.0177	0.0205
4.0		0.9839	0.9863	0.9897	0.9930	0.9955		0.0033	0.0058	0.0067
4.5		0.9953	0.9961	0.9971	0.9982	0.9990		0.0011	0.0019	0.0021
5.0		1.0	1.0	0.9999	0.9999	0.9999		0	0	0
5.5		1.0	1.0	1.0	1.0	1.0		0	0	0

Note: ϑ_1 is zero for θ_e = 0° and 90°.

TABLE 14/

TABLE 14

Primary and secondary flow profiles with a positive pressure gradient and suction

$K = 0.4, \quad \beta = -0.35$

$\theta_e \rightarrow$	0°	15°	30°	45°	60°	75°	90°	15°,75°	30°,60°	45°
Y	$\frac{u_1}{U_1}=\frac{u}{U}$	$\frac{u_1}{U_1}$	$\frac{u_1}{U_1}$	$\frac{u_1}{U_1}$	$\frac{u_1}{U_1}$	$\frac{u_1}{U_1}$	$\frac{u_1}{U_1}=\frac{\vartheta}{V_o}$	$\frac{\vartheta_1}{U_1}$	$\frac{\vartheta_1}{U_1}$	$\frac{\vartheta_1}{U_1}$
0		0	0	0	0	0		0	0	0
0.5		0.1293	0.1630	0.2089	0.2549	0.2886		0.0460	0.0796	0.0919
1.0		0.3061	0.3527	0.4164	0.4802	0.5268		0.0637	0.1104	0.1274
1.5	Reference (10)	0.5061	0.5501	0.6101	0.6702	0.7142	Reference (11)	0.0601	0.1040	0.1201
2.0		0.6957	0.7279	0.7717	0.8156	0.8477		0.0439	0.0760	0.0877
2.5		0.8438	0.8623	0.8875	0.9128	0.9313		0.0253	0.0438	0.0505
3.0		0.9350	0.9471	0.9547	0.9660	0.9744		0.0113	0.0196	0.0227
3.5		0.9781	0.9811	0.9851	0.9892	0.9922		0.0041	0.0070	0.0081
4.0		0.9943	0.9950	0.9960	0.9970	0.9977		0.0010	0.0017	0.0020
4.5		0.9990	0.9991	0.9991	0.9992	0.9993		0.0001	0.0001	0.0001
5.0		1.0	1.0	1.0	1.0	1.0		0	0	0

Note: ϑ_1 is zero for $\theta_e = 0°$ and $90°$.

TABLE 15

Primary and secondary flow profiles with a positive pressure gradient and suction (separation case)

$K = 0.6, \quad \beta = -0.474$

$\theta_e \rightarrow$	0°	15°	30°	45°	60°	75°	90°	15°,75°	30°,60°	45°
Y	$\frac{u_1}{U_1}=\frac{u}{U}$	$\frac{u_1}{U_1}$	$\frac{u_1}{U_1}$	$\frac{u_1}{U_1}$	$\frac{u_1}{U_1}$	$\frac{u_1}{U_1}$	$\frac{u_1}{U_1}=\frac{\vartheta}{V_o}$	$\frac{\vartheta_1}{U_1}$	$\frac{\vartheta_1}{U_1}$	$\frac{\vartheta_1}{U_1}$
0		0	0	0	0	0		0	0	0
0.5		0.0729	0.1244	0.1948	0.2652	0.3167		0.0704	0.1219	0.1408
1.0		0.2210	0.2919	0.3888	0.4857	0.5566		0.0969	0.1678	0.1938
1.5	Reference (10)	0.4156	0.4830	0.5750	0.6667	0.7343	Reference (11)	0.0920	0.1593	0.1840
2.0		0.6204	0.6706	0.7392	0.8078	0.8580		0.0686	0.1188	0.1372
2.5		0.7939	0.8236	0.8643	0.9049	0.9347		0.0406	0.0704	0.0813
3.0		0.9091	0.9230	0.9420	0.9610	0.9749		0.0190	0.0329	0.0380
3.5		0.9688	0.9737	0.9805	0.9872	0.9922		0.0067	0.0117	0.0135
4.0		0.9915	0.9929	0.9947	0.9966	0.9980		0.0019	0.0032	0.0037
4.5		0.9981	0.9984	0.9988	0.9993	0.9996		0.0004	0.0007	0.0008
5.0		1.0	1.0	0.9999	0.9999	0.9999		0	0	0
5.5		1.0	1.0	1.0	1.0	1.0		0	0	0

Note: ϑ_1 is zero for $\theta_e = 0°$ and $90°$.

TABLE 16/

TABLE 16

Primary and secondary flow profiles with a positive pressure gradient and suction

$K = 0.6, \quad \beta = -0.35$

$\theta_e \rightarrow$	0°	15°	30°	45°	60°	75°	90°	15°,75°	30°,60°	45°
Y	$\frac{u_1}{U_1}=\frac{u}{U}$	$\frac{u_1}{U_1}$	$\frac{u_1}{U_1}$	$\frac{u_1}{U_1}$	$\frac{u_1}{U_1}$	$\frac{u_1}{U_1}$	$\frac{u_1}{U_1}=\frac{\vartheta}{V_o}$	$\frac{\vartheta_1}{U_1}$	$\frac{\vartheta_1}{U_1}$	$\frac{\vartheta_1}{U_1}$
0		0	0	0	0	0		0	0	0
0.5	Reference (10)	0.2568	0.2808	0.3136	0.3465	0.3705	Reference (11)	0.0328	0.0568	0.0656
1.0		0.5045	0.5332	0.5724	0.6116	0.6403		0.0392	0.0679	0.0784
1.5		0.7151	0.7373	0.7677	0.7980	0.8203		0.0303	0.0526	0.0607
2.0		0.8637	0.8765	0.8939	0.9114	0.9242		0.0175	0.0303	0.0349
2.5		0.9471	0.9527	0.9604	0.9681	0.9737		0.0077	0.0133	0.0154
3.0		0.9828	0.9848	0.9877	0.9905	0.9926		0.0028	0.0049	0.0057
3.5		0.9952	0.9959	0.9968	0.9977	0.9984		0.0009	0.0015	0.0018
4.0		0.9990	0.9992	0.9994	0.9996	0.9997		0	0	0
4.5		1.0	1.0	1.0	1.0	1.0		0	0	0

Note: ϑ_1 is zero for $\theta_e = 0°$ and $90°$

TABLE 17

Primary and secondary flow profiles with a positive pressure gradient and suction (separation case)

$K = 0.8, \quad \beta = -0.592$

$\theta_e \rightarrow$	0°	15°	30°	45°	60°	75°	90°	15°,75°	30°,60°	45°
Y	$\frac{u_1}{U_1}=\frac{u}{U}$	$\frac{u_1}{U_1}$	$\frac{u_1}{U_1}$	$\frac{u_1}{U_1}$	$\frac{u_1}{U_1}$	$\frac{u_1}{U_1}$	$\frac{u_1}{U_1}=\frac{\vartheta}{V_o}$	$\frac{\vartheta_1}{U_1}$	$\frac{\vartheta_1}{U_1}$	$\frac{\vartheta_1}{U_1}$
0		0	0	0	0	0		0	0	0
0.5	Reference (10)	0.0868	0.1464	0.2277	0.3091	0.3687	Reference (11)	0.0814	0.1409	0.1627
1.0		0.2563	0.3336	0.4391	0.5447	0.6220		0.1056	0.1828	0.2111
1.5		0.4681	0.5366	0.6301	0.7237	0.7922		0.0936	0.1621	0.1871
2.0		0.6772	0.7240	0.7881	0.8521	0.8990		0.0640	0.1109	0.1281
2.5		0.8401	0.8651	0.8992	0.9333	0.9583		0.0341	0.0591	0.0682
3.0		0.9368	0.9471	0.9613	0.9754	0.9858		0.0141	0.0245	0.0283
3.5		0.9802	0.9836	0.9881	0.9927	0.9961		0.0046	0.0079	0.0091
4.0		0.9953	0.9961	0.9972	0.9983	0.9991		0.0011	0.0019	0.0022
4.5		0.9991	0.9992	0.9994	0.9997	0.9998		0.00025	0.0004	0.00045
5.0		1.0	1.0	1.0	1.0	1.0		0	0	0

Note: ϑ_1 is zero for $\theta_e = 0°$ and $90°$.

TABLE 18/

TABLE 18

Primary and secondary flow profiles with a positive pressure gradient and suction

$K = 0.8, \quad \beta = -0.50$

$\theta_e \rightarrow$		0°	15°	30°	45°	60°	75°	90°		15°,75°	30°,60°	45°
Y		$\frac{u_1}{U_1}=\frac{u}{U}$	$\frac{u_1}{U_1}$	$\frac{u_1}{U_1}$	$\frac{u_1}{U_1}$	$\frac{u_1}{U_1}$	$\frac{u_1}{U_1}$	$\frac{u_1}{U_1}=\frac{\vartheta}{V_o}$		$\frac{\vartheta_1}{U_1}$	$\frac{\vartheta_1}{U_1}$	$\frac{\vartheta_1}{U_1}$
0			0	0	0	0	0			0	0	0
0.5			0.2495	0.2838	0.3306	0.3774	0.4116			0.0468	0.0810	0.0936
1.0	Reference (10)		0.4984	0.5379	0.5917	0.6456	0.6850	Reference (11)		0.0539	0.0933	0.1077
1.5			0.7137	0.7431	0.7831	0.8232	0.8526			0.0401	0.0694	0.0801
2.0			0.8659	0.8819	0.9038	0.9258	0.9418			0.0219	0.0380	0.0438
2.5			0.9494	0.9562	0.9653	0.9745	0.9812			0.0092	0.0159	0.0183
3.0			0.9848	0.9870	0.9900	0.9930	0.9952			0.0030	0.0052	0.0060
4.0			0.9962	0.9968	0.9976	0.9985	0.9991			0.0008	0.0014	0.0016
4.5			0.9991	0.9992	0.9995	0.9997	0.9999			0.00025	0.0004	0.0005
5.0			1.0	1.0	1.0	1.0	1.0			0	0	0

Note: ϑ_1 is zero for $\theta_e = 0°$ and 90°.

TABLE 19

Primary and secondary flow profiles with a positive pressure gradient and suction (separation case)

$K = 1.0, \quad \beta = -0.721$

$\theta_e \rightarrow$		0°	15°	30°	45°	60°	75°	90°		15°,75°	30°,60°	45°
Y		$\frac{u_1}{U_1}=\frac{u}{U}$	$\frac{u_1}{U_1}$	$\frac{u_1}{U_1}$	$\frac{u_1}{U_1}$	$\frac{u_1}{U_1}$	$\frac{u_1}{U_1}$	$\frac{u_1}{U_1}=\frac{\vartheta}{V_o}$		$\frac{\vartheta_1}{U_1}$	$\frac{\vartheta_1}{U_1}$	$\frac{\vartheta_1}{U_1}$
0			0	0	0	0	0			0	0	0
0.5			0.1015	0.1684	0.2597	0.3511	0.4180			0.0914	0.1583	0.1827
1.0			0.2919	0.3737	0.4853	0.5970	0.6788			0.1117	0.1934	0.2233
1.5	Reference (10)		0.5196	0.5868	0.6787	0.7705	0.8378	Reference (11)		0.0918	0.1591	0.1837
2.0			0.7294	0.7714	0.8288	0.8862	0.9282			0.0574	0.0994	0.1148
2.5			0.8783	0.8974	0.9257	0.9531	0.9732			0.0274	0.0474	0.0547
3.0			0.9576	0.9648	0.9747	0.9845	0.9918			0.0098	0.0171	0.0197
3.5			0.9887	0.9906	0.9932	0.9959	0.9978			0.0026	0.0045	0.0052
4.0			0.9981	0.9984	0.9987	0.9991	0.9994			0.0004	0.0006	0.0007
4.5			1.0	0.9999	0.9998	0.9998	0.9997			0	0	0
5.0			1.0	0.9999	0.9999	0.9998	0.9998			0	0	0
5.5			1.0	1.0	1.0	1.0	1.0			0	0	0

Note: ϑ_1 is zero for $\theta_e = 0°$ and 90°.

TABLE 20/

TABLE 20

Primary and secondary flow profiles with a positive pressure gradient and suction

K = 1.0, β = - 0.60

$\theta_e \rightarrow$		0°	15°	30°	45°	60°	75°	90°		15°,75°	30°,60°	45°
Y		$\frac{u_1}{U_1}=\frac{u}{U}$	$\frac{u_1}{U_1}$	$\frac{u_1}{U_1}$	$\frac{u_1}{U_1}$	$\frac{u_1}{U_1}$	$\frac{u_1}{U_1}$	$\frac{u_1}{U_1}=\frac{v}{V_o}$		$\frac{v_1}{U_1}$	$\frac{v_1}{U_1}$	$\frac{v_1}{U_1}$
0		0	0	0	0	0	0			0	0	0
0.5		0.2903	0.3265	0.3761	0.4256	0.4619				0.0495	0.0858	0.0991
1.0	Reference (10)	0.5571	0.5955	0.6479	0.7004	0.7388		Reference (11)		0.0525	0.0909	0.1049
1.5		0.7684	0.7942	0.8294	0.8647	0.8905				0.0352	0.0610	0.0704
2.0		0.9026	0.9151	0.9322	0.9494	0.9619				0.0171	0.0297	0.0342
2.5		0.9677	0.9723	0.9786	0.9849	0.9895				0.0063	0.0109	0.0126
3.0		0.9915	0.9930	0.9946	0.9965	0.9978				0.0018	0.0032	0.0036
3.5		0.9981	0.9985	0.9990	0.9995	0.9999				0.0005	0.0009	0.0010
4.0		1.0	1.0	1.0	1.0	1.0				0	0	0
4.5		1.0	1.0	1.0	1.0	1.0				0	0	0

Note: ϑ_1 is zero for θ_e = 0° and 90°.

TABLE 21

Primary and secondary flow profiles with a positive pressure gradient and suction (separation case)

K = 1.414, β = - 1.0

$\theta_e \rightarrow$		0°	15°	30°	45°	60°	75°	90°		15°,75°	30°,60°	45°
Y		$\frac{u_1}{U_1}=\frac{u}{U}$	$\frac{u_1}{U_1}$	$\frac{u_1}{U_1}$	$\frac{u_1}{U_1}$	$\frac{u_1}{U_1}$	$\frac{u_1}{U_1}$	$\frac{u_1}{U_1}=\frac{v}{V_o}$		$\frac{v_1}{U_1}$	$\frac{v_1}{U_1}$	$\frac{v_1}{U_1}$
0		0	0	0	0	0	0			0	0	0
0.25		0.0473	0.1002	0.1724	0.2447	0.2975				0.0722	0.1251	0.1444
0.50		0.1294	0.2099	0.3198	0.4297	0.5101				0.1099	0.1903	0.2198
0.75		0.2350	0.3252	0.4483	0.5715	0.6617				0.1232	0.2133	0.2463
1.0		0.3551	0.4428	0.5626	0.6825	0.7702				0.1198	0.2075	0.2396
1.25		0.4794	0.5572	0.6633	0.7695	0.8472				0.1062	0.1839	0.2123
1.50	Reference (10)	0.6003	0.6639	0.7507	0.8376	0.9012		Reference (11)		0.0869	0.1505	0.1737
1.75		0.7087	0.7572	0.8234	0.8897	0.9382				0.0662	0.1147	0.1324
2.0		0.7996	0.8341	0.8812	0.9283	0.9628				0.0471	0.0816	0.0942
2.25		0.8704	0.8932	0.9244	0.9557	0.9735				0.0312	0.0541	0.0624
2.50		0.9221	0.9361	0.9552	0.9743	0.9883				0.0191	0.0331	0.0382
2.75		0.9559	0.9639	0.9749	0.9858	0.9939				0.0109	0.0190	0.0219
3.0		0.9766	0.9809	0.9868	0.9927	0.9970				0.0059	0.0102	0.0118
3.25		0.9888	0.9908	0.9937	0.9965	0.9986				0.0028	0.0049	0.0057
3.50		0.9944	0.9954	0.9968	0.9983	0.9993				0.0014	0.0025	0.0028
3.75		0.9972	0.9977	0.9984	0.9992	0.9997				0.0007	0.0012	0.0014
4.0		0.9991	0.9992	0.9995	0.9997	0.9999				0.0002	0.0004	0.0005
4.25		1.0	1.0	1.0	1.0	1.0				0	0	0

Note: ϑ_1 is zero for θ_e = 0° and 90°.

TABLE 22/

TABLE 22

Primary and secondary flow profiles with a positive pressure gradient and suction

$K = 1.554, \beta = -1.0$

$\theta_e \rightarrow$		0°	15°	30°	45°	60°	75°		90°	15°,75°	30°,60°	45°
Y		$\frac{u_1}{U_1}=\frac{u}{U}$	$\frac{u_1}{U_1}$	$\frac{u_1}{U_1}$	$\frac{u_1}{U_1}$	$\frac{u_1}{U_1}$	$\frac{u_1}{U_1}$		$\frac{u_1}{U_1}=\frac{\vartheta}{V_o}$	$\frac{\vartheta_1}{U_1}$	$\frac{\vartheta_1}{U_1}$	$\frac{\vartheta_1}{U_1}$
0		0	0	0	0	0	0			0	0	0
0.25		0.1738	0.2089	0.2568	0.3048	0.3398				0.0479	0.0830	0.0958
0.50		0.3372	0.3869	0.4548	0.5228	0.5725				0.0679	0.1176	0.1358
0.75		0.4887	0.5396	0.6092	0.6789	0.7298				0.0696	0.1206	0.1392
1.0		0.6233	0.6680	0.7290	0.7900	0.8346				0.0610	0.1056	0.1220
1.25		0.7359	0.7711	0.8191	0.8672	0.9024				0.0481	0.0833	0.0961
1.50	Reference (10)	0.8262	0.8512	0.8855	0.9197	0.9448		Reference (11)		0.0342	0.0593	0.0685
1.75		0.8920	0.9086	0.9311	0.9537	0.9702				0.0226	0.0391	0.0451
2.0		0.9376	0.9476	0.9612	0.9748	0.9847				0.0136	0.0235	0.0272
2.25		0.9660	0.9716	0.9793	0.9869	0.9925				0.0076	0.0132	0.0153
2.50		0.9830	0.9859	0.9898	0.9938	0.9966				0.0039	0.0068	0.0078
2.75		0.9915	0.9930	0.9950	0.9970	0.9985				0.0020	0.0035	0.0040
3.0		0.9962	0.9969	0.9978	0.9987	0.9994				0.0009	0.0015	0.0018
3.25		0.9981	0.9985	0.9989	0.9994	0.9998				0.0005	0.0008	0.0009
3.50		0.9991	0.9992	0.9995	0.9997	0.9999				0.0002	0.0004	0.0005
3.75		1.0	1.0	1.0	1.0	1.0				0	0	0
4.0		1.0	1.0	1.0	1.0	1.0				0	0	0

Note: ϑ_1 is zero for $\theta_e = 0°$ and $90°$.

TABLE 23/

TABLE 23

Primary and secondary flow profiles with infinitely large positive pressure gradient and suction (separation case)

$K = 2.828, \quad \beta = -\infty$

$\theta_e \rightarrow$		0°	15°	30°	45°	60°	75°	90°		15°,75°	30°,60°	45°
η		$\frac{u_1}{U_1}=\frac{u}{U}$	$\frac{u_1}{U_1}$	$\frac{u_1}{U_1}$	$\frac{u_1}{U_1}$	$\frac{u_1}{U_1}$	$\frac{u_1}{U_1}$	$\frac{u_1}{U_1}=\frac{\vartheta}{V_o}$		$\frac{\vartheta_1}{U_1}$	$\frac{\vartheta_1}{U_1}$	$\frac{\vartheta_1}{U_1}$
0		0	0	0	0	0	0			0		
0.027		0.0516	0.0559	0.0617	0.0676	0.0719				0.0059	0.0102	0.0117
0.055		0.1029	0.1110	0.1220	0.1330	0.1410				0.0110	0.0190	0.0220
0.086		0.1544	0.1665	0.1829	0.1994	0.2115				0.0165	0.0285	0.0329
0.119		0.2057	0.2214	0.2428	0.2643	0.2800				0.0214	0.0371	0.0428
0.154		0.2569	0.2758	0.3015	0.3273	0.3462				0.0258	0.0446	0.0515
0.192		0.3080	0.3297	0.3595	0.3892	0.4110				0.0297	0.0515	0.0595
0.234		0.3590	0.3835	0.4170	0.4505	0.4750				0.0335	0.0580	0.0670
0.279	Reference (10)	0.4097	0.4364	0.4728	0.5093	0.5359			Reference (11)	0.0364	0.0631	0.0728
0.329		0.4604	0.4889	0.5278	0.5667	0.5952				0.0389	0.0674	0.0778
0.385		0.5109	0.5408	0.5817	0.6225	0.6524				0.0408	0.0707	0.0817
0.447		0.5612	0.5919	0.6337	0.6756	0.7063				0.0419	0.0725	0.0837
0.518		0.6113	0.6422	0.6844	0.7267	0.7576				0.0422	0.0731	0.0844
0.600		0.6612	0.6917	0.7333	0.7750	0.8055				0.0417	0.0722	0.0833
0.695		0.7107	0.7400	0.7799	0.8199	0.8492				0.0400	0.0692	0.0799
0.811		0.7600	0.7873	0.8245	0.8618	0.8891				0.0373	0.0646	0.0745
0.954		0.8089	0.8332	0.8663	0.8995	0.9238				0.0332	0.0574	0.0663
1.143		0.8574	0.8776	0.9052	0.9329	0.9531				0.0276	0.0478	0.0552
1.414		0.9055	0.9204	0.9408	0.9613	0.9762				0.0204	0.0354	0.0408
1.889		0.9530	0.9613	0.9726	0.9839	0.9922				0.0113	0.0196	0.0226
∞		1.0	1.0	1.0	1.0	1.0				0	0	0

Note: ϑ_1 is zero for $\theta_e = 0°$ and 90°.

TABLE 24/

TABLE 24

Primary and secondary flow profiles with an infinitely large positive pressure gradient and large suction

$K = 3.6, \quad \beta = -\infty$

$\theta_e \rightarrow$	0°	15°	30°	45°	60°	75°	90°	15°,75°	30°,60°	45°
η	$\frac{u_1}{U_1}=\frac{l}{U}$	$\frac{u_1}{U_1}$	$\frac{u_1}{U_1}$	$\frac{u_1}{U_1}$	$\frac{u_1}{U_1}$	$\frac{u_1}{U_1}$	$\frac{u_1}{U_1}-\frac{\vartheta}{V_o}$	$\frac{\vartheta_1}{U_1}$	$\frac{\vartheta_1}{U_1}$	$\frac{\vartheta_1}{U_1}$
0		0	0	0	0	0		0	0	0
0.016		0.0504	0.0516	0.0533	0.0549	0.0562		0.00165	0.00286	0.00330
0.033		0.1009	0.1032	0.1065	0.1097	0.1121		0.00325	0.00563	0.00650
0.051		0.1512	0.1547	0.1593	0.1640	0.1674		0.00467	0.00810	0.00935
0.071		0.2016	0.2061	0.2122	0.2184	0.2229		0.00612	0.01061	0.01225
0.091		0.2520	0.2575	0.2649	0.2724	0.2779		0.00747	0.01295	0.01495
0.113		0.3023	0.3087	0.3173	0.3260	0.3324		0.00867	0.01502	0.01735
0.137	Reference (10)	0.3526	0.3599	0.3698	0.3797	0.3869	Reference (11)	0.00990	0.01715	0.01980
0.163		0.4029	0.4108	0.4215	0.4323	0.4402		0.01077	0.01866	0.02155
0.191		0.4531	0.4617	0.4733	0.4850	0.4936		0.01167	0.02022	0.02335
0.221		0.5033	0.5124	0.5247	0.5371	0.5462		0.01237	0.02143	0.02475
0.256		0.5535	0.5629	0.5758	0.5888	0.5982		0.01292	0.02239	0.02585
0.294		0.6036	0.6133	0.6265	0.6398	0.6495		0.01327	0.02299	0.02655
0.337		0.6536	0.6633	0.6766	0.6900	0.6997		0.01332	0.02308	0.02665
0.388		0.7035	0.7131	0.7262	0.7394	0.7490		0.01312	0.02273	0.02625
0.448		0.7534	0.7626	0.7752	0.7879	0.7971		0.01262	0.02187	0.02525
0.521		0.8031	0.8117	0.8234	0.8352	0.8438		0.01172	0.02031	0.02345
0.616		0.8528	0.8603	0.8706	0.8810	0.8889		0.01032	0.01788	0.02065
0.752		0.9022	0.9083	0.9166	0.9249	0.9310		0.00830	0.01437	0.01660
0.985		0.9514	0.9553	0.9606	0.9660	0.9697		0.00532	0.00922	0.01065
∞		1.0	1.0	1.0	1.0	1.0		0	0	0

Note: ϑ_1 is zero for $\theta_e = 0°$ and $90°$.

HBF

Fig 1

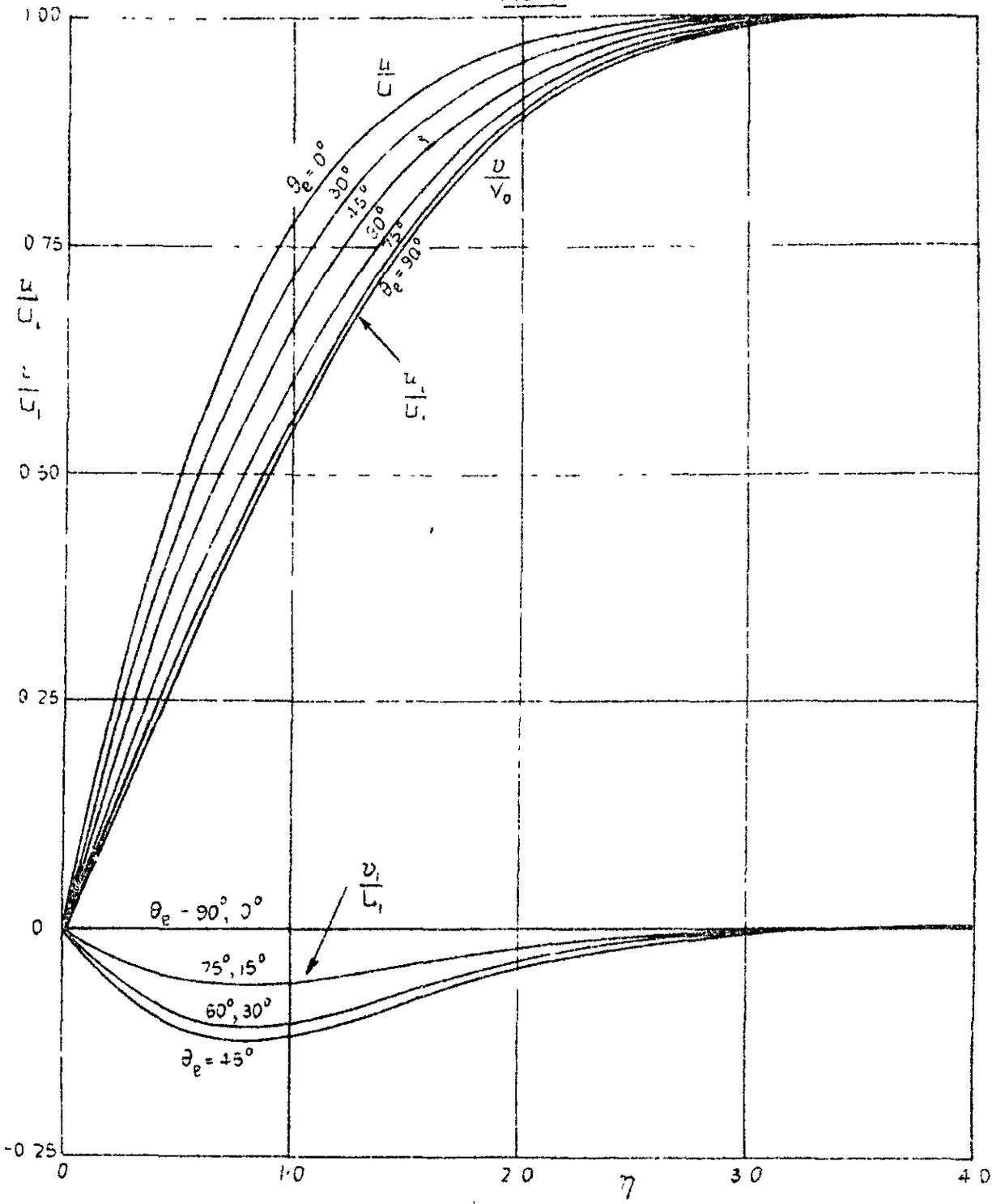

Primary and secondary flow profiles for the stagnation flow with zero suction ($K = 0$, $\beta = 1$)

FIG 2

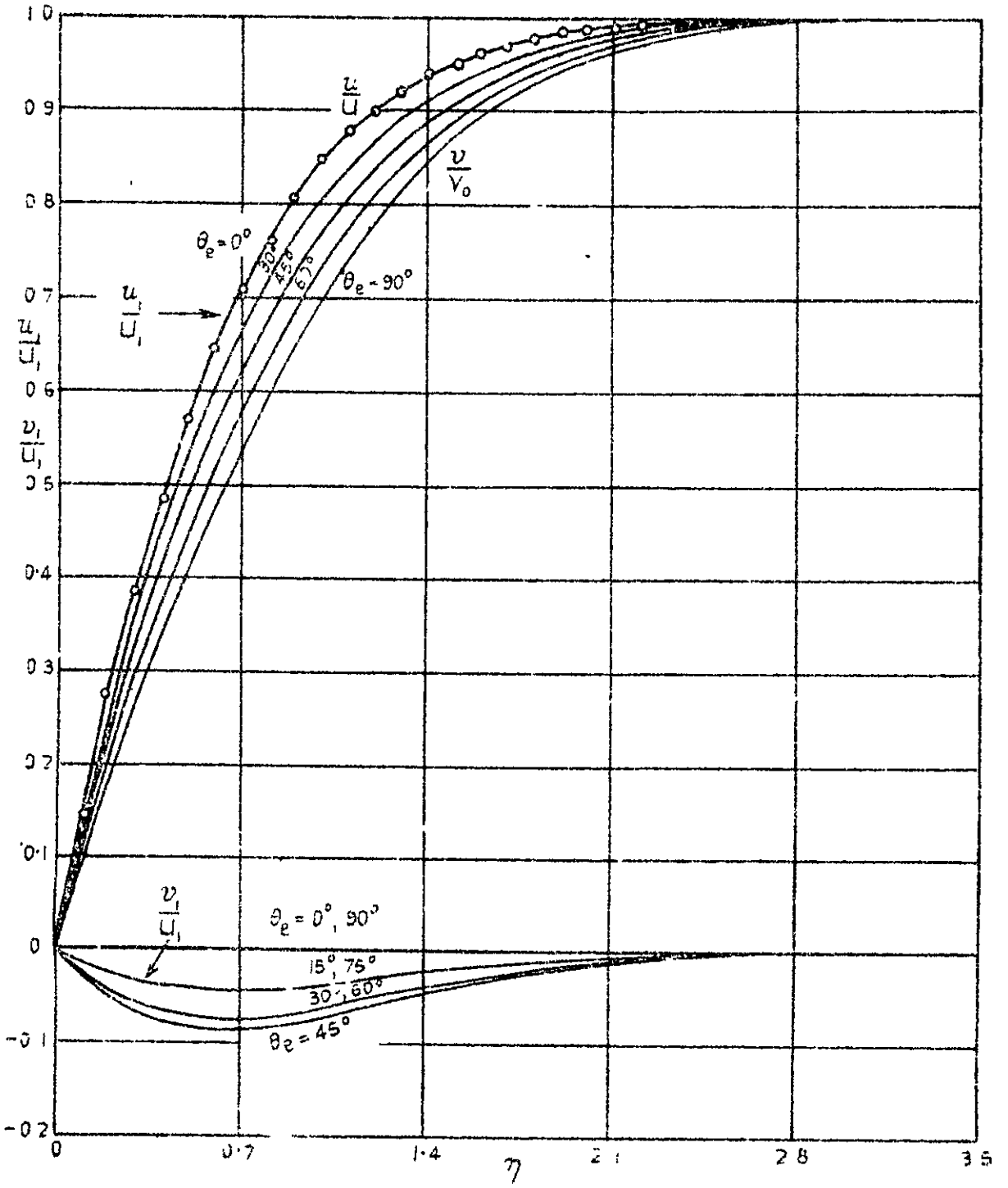

Primary and secondary flow profiles for the stagnation flow with suction ($K = 0.5$, $\beta = 1$)

FIG 3

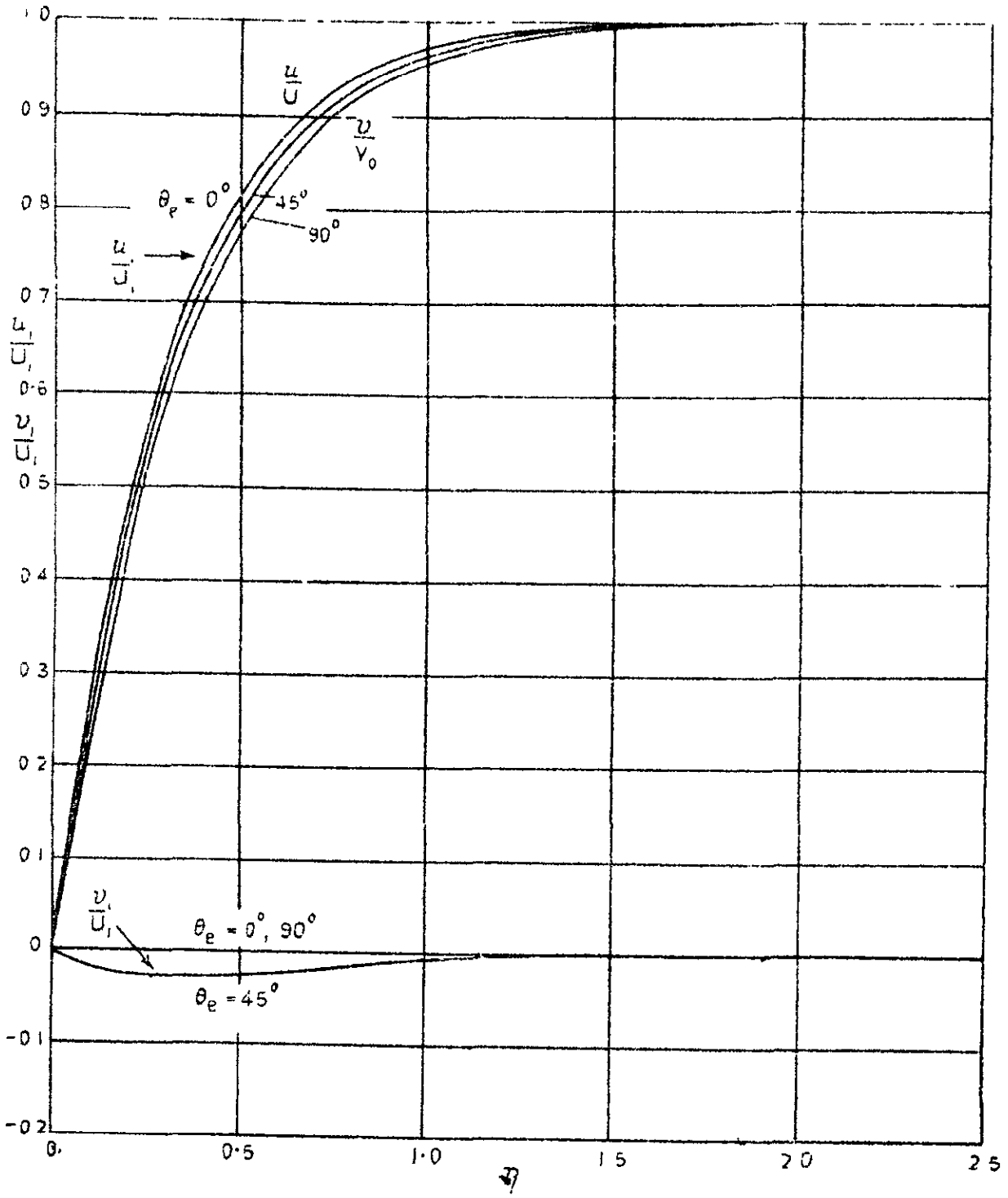

Primary and secondary flow profiles for the stagnation flow with suction ($K = 2{\cdot}664$, $\beta = 1$)

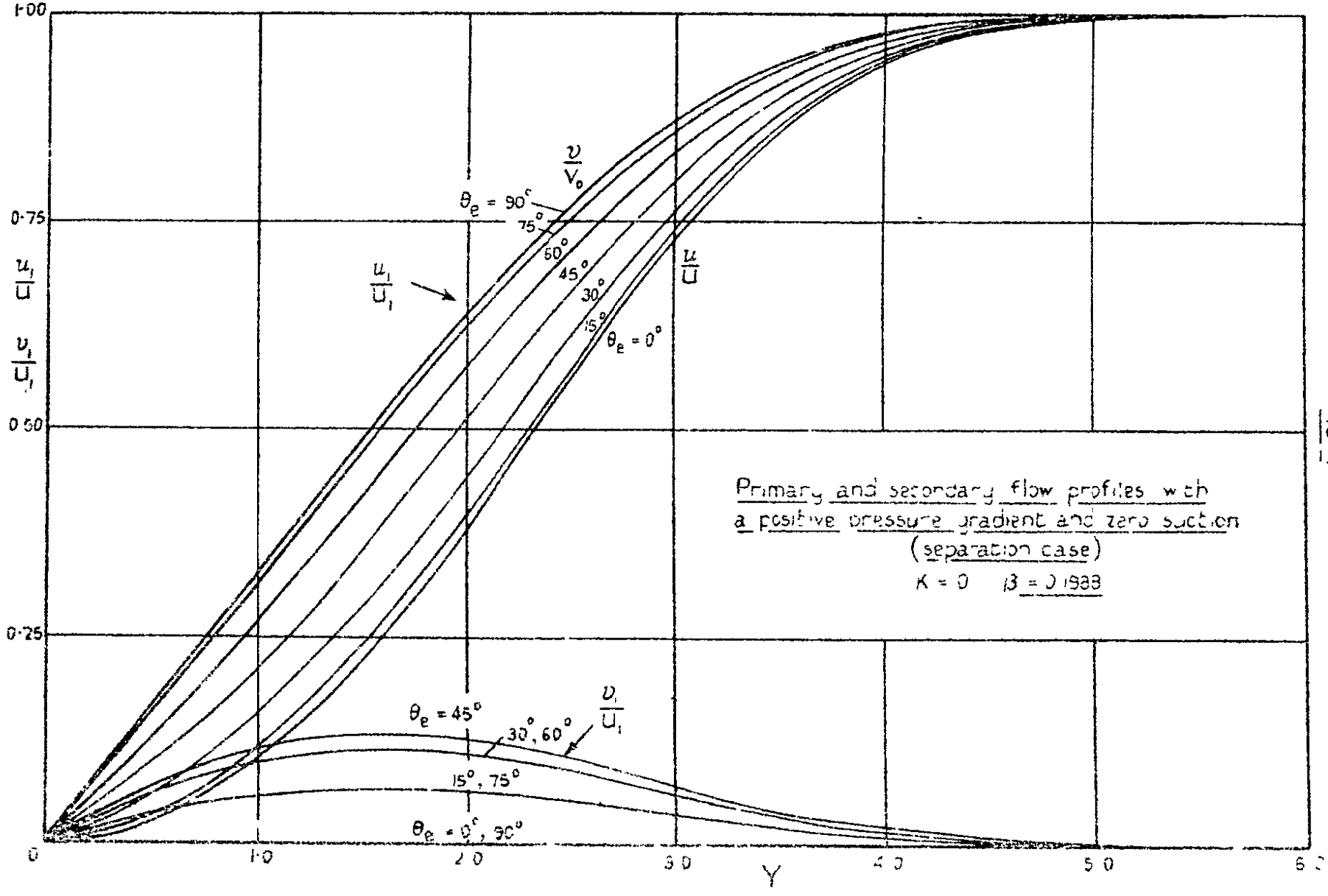
1·00
0·75
0·50
0·25
0
1·0
2·0
3·0
4·0
5·0
Y
$\frac{u_1}{U_1}$
$\frac{v_1}{U_1}$
$\frac{v}{V_0}$
$\frac{u}{U}$
$\theta_e = 90°$
75°
60°
45°
30°
15°
$\theta_e = 0°$
$\theta_e = 45°$
30°, 60°
15°, 75°
$\theta_e = 0°, 90°$
Primary and secondary flow profiles with a positive pressure gradient and zero suction
(separation case)
K = 0 β = 0·1988

Fig 4

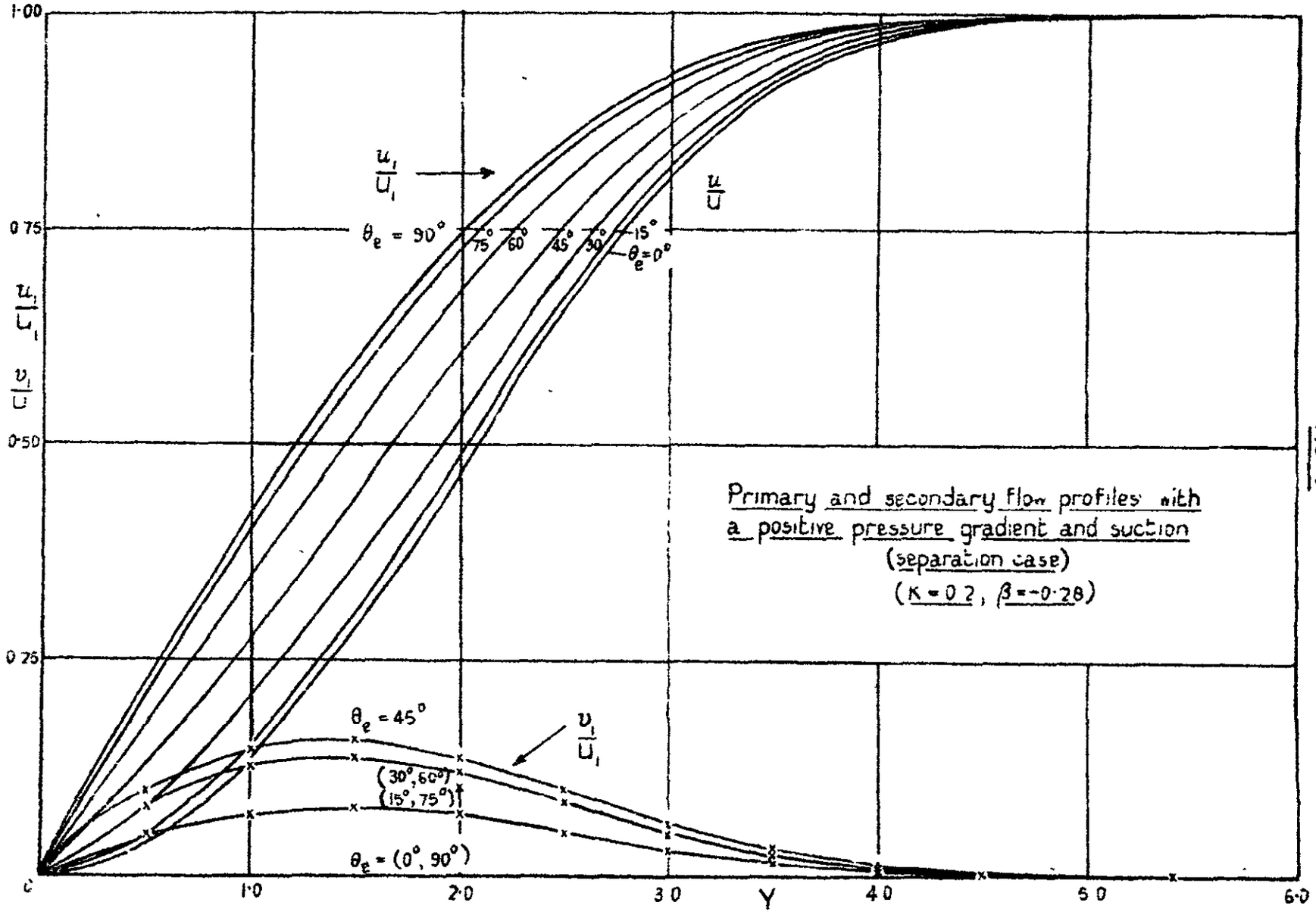
1·00
0·75
0·50
0·25
0
$\frac{u_1}{U_1}$
$\frac{v_1}{U}$
$\frac{u_1}{U_1}$
$\theta_e = 90°$
75°
60°
45°
30°
15°
$\theta_e = 0°$
$\frac{u}{U}$
$\theta_e = 45°$
$\frac{v_1}{U_1}$
(30°, 60°)
(15°, 75°)
$\theta_e = (0°, 90°)$
1·0
2·0
3·0
Y
4·0
5·0
6·0
Primary and secondary flow profiles with a positive pressure gradient and suction (separation case)
(K = 0·2, β = −0·28)

FIG. 5

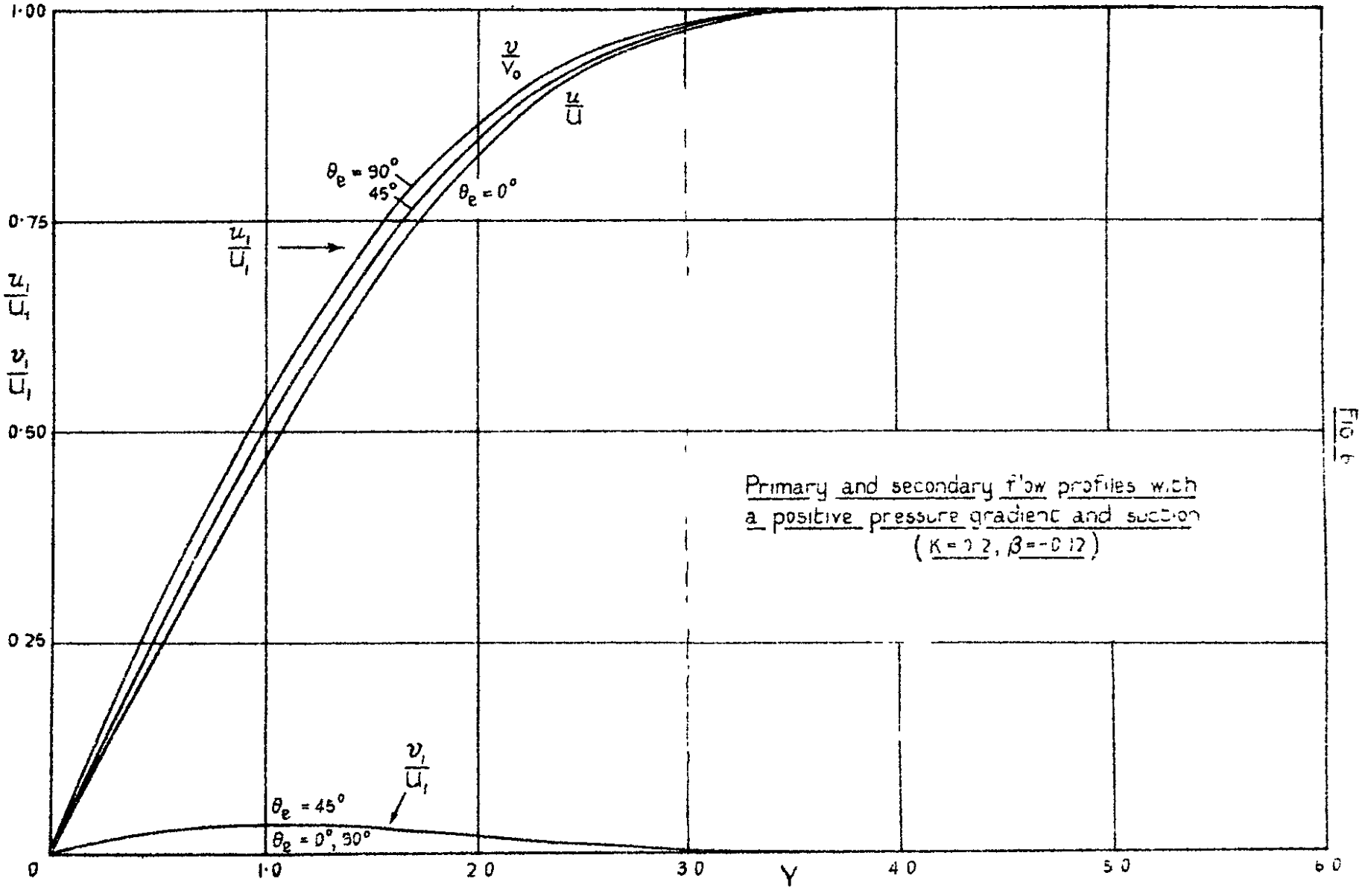

Primary and secondary flow profiles with a positive pressure gradient and suction
(K = 2 2, β = -0 12)

Fig 7

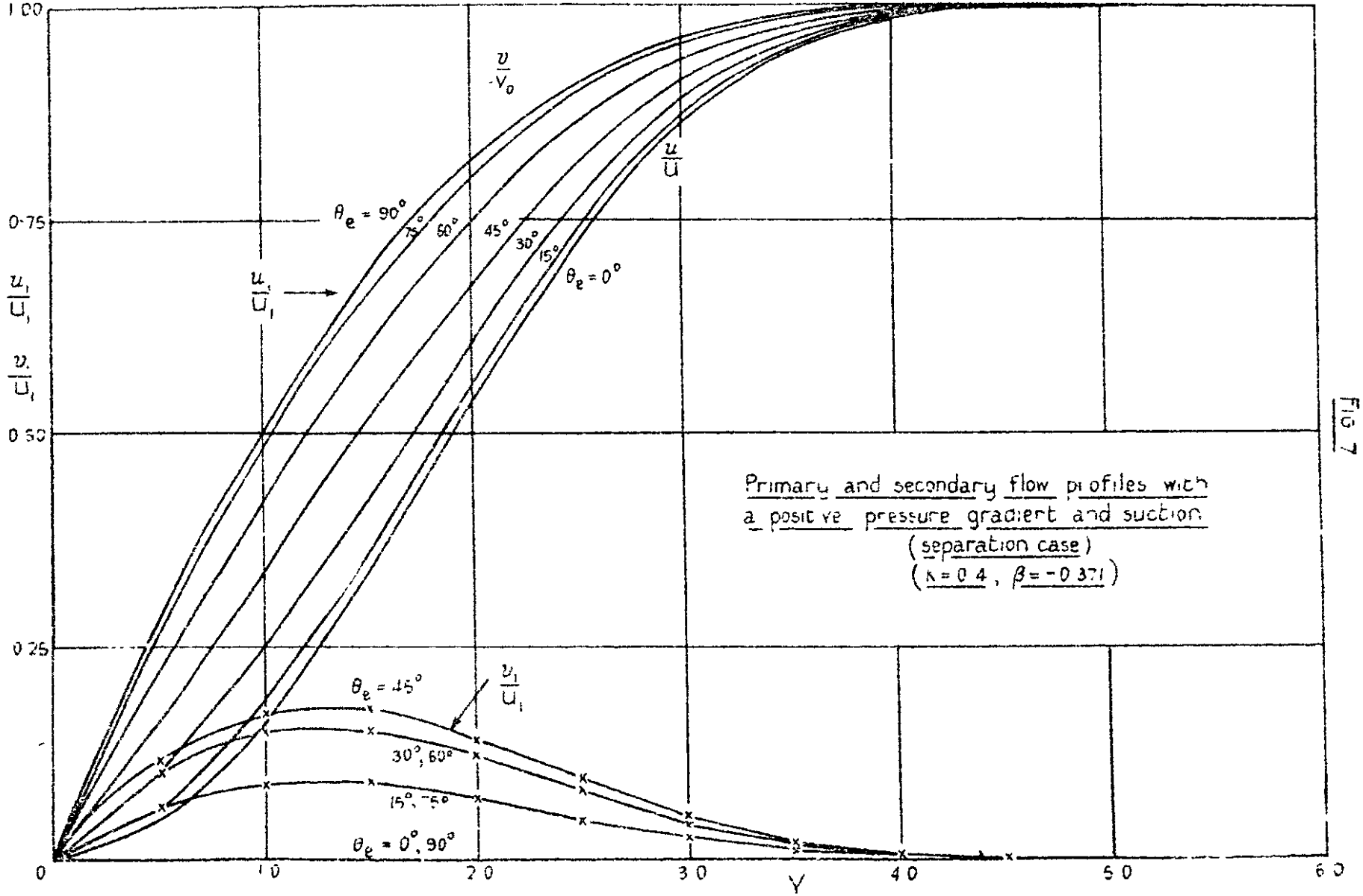
1·00
0·75
0·50
0·25
0
$\frac{u_1}{U_1}$
$\frac{v_1}{U_1}$
$\frac{v}{V_0}$
$\frac{u}{U}$
$\theta_e = 90°$
75°
60°
45°
30°
15°
$\theta_e = 0°$
$\frac{u_1}{U_1}$
$\frac{v_1}{U_1}$
$\theta_e = 45°$
30°, 60°
15°, 75°
$\theta_e = 0°, 90°$
10
20
30
40
50
60
Y
Primary and secondary flow profiles with a positive pressure gradient and suction
(separation case)
(K = 0·4, β = −0·371)

FIG 7

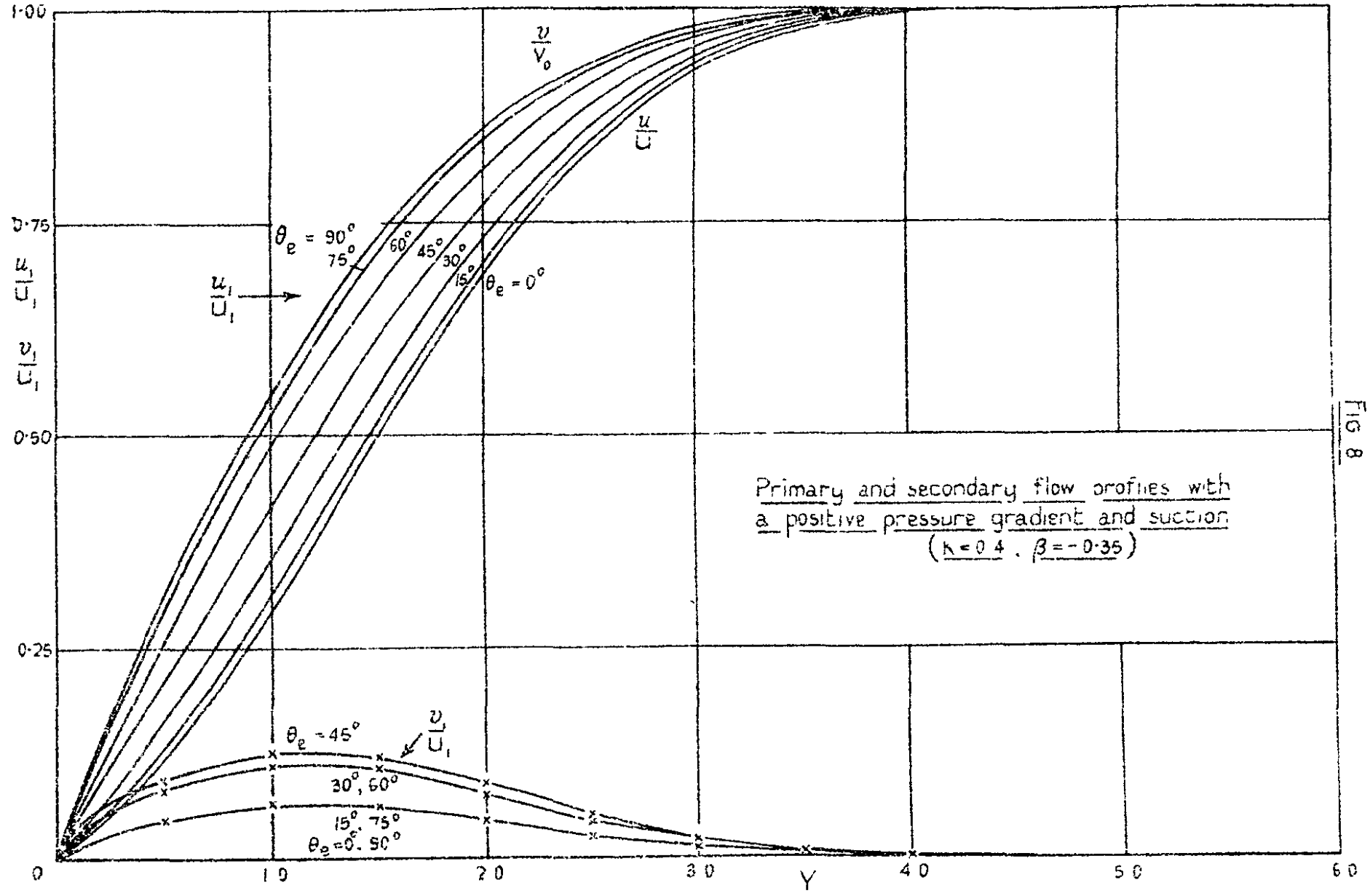

Primary and secondary flow profiles with a positive pressure gradient and suction
($k = 0.4$, $\beta = -0.35$)

Fig 8

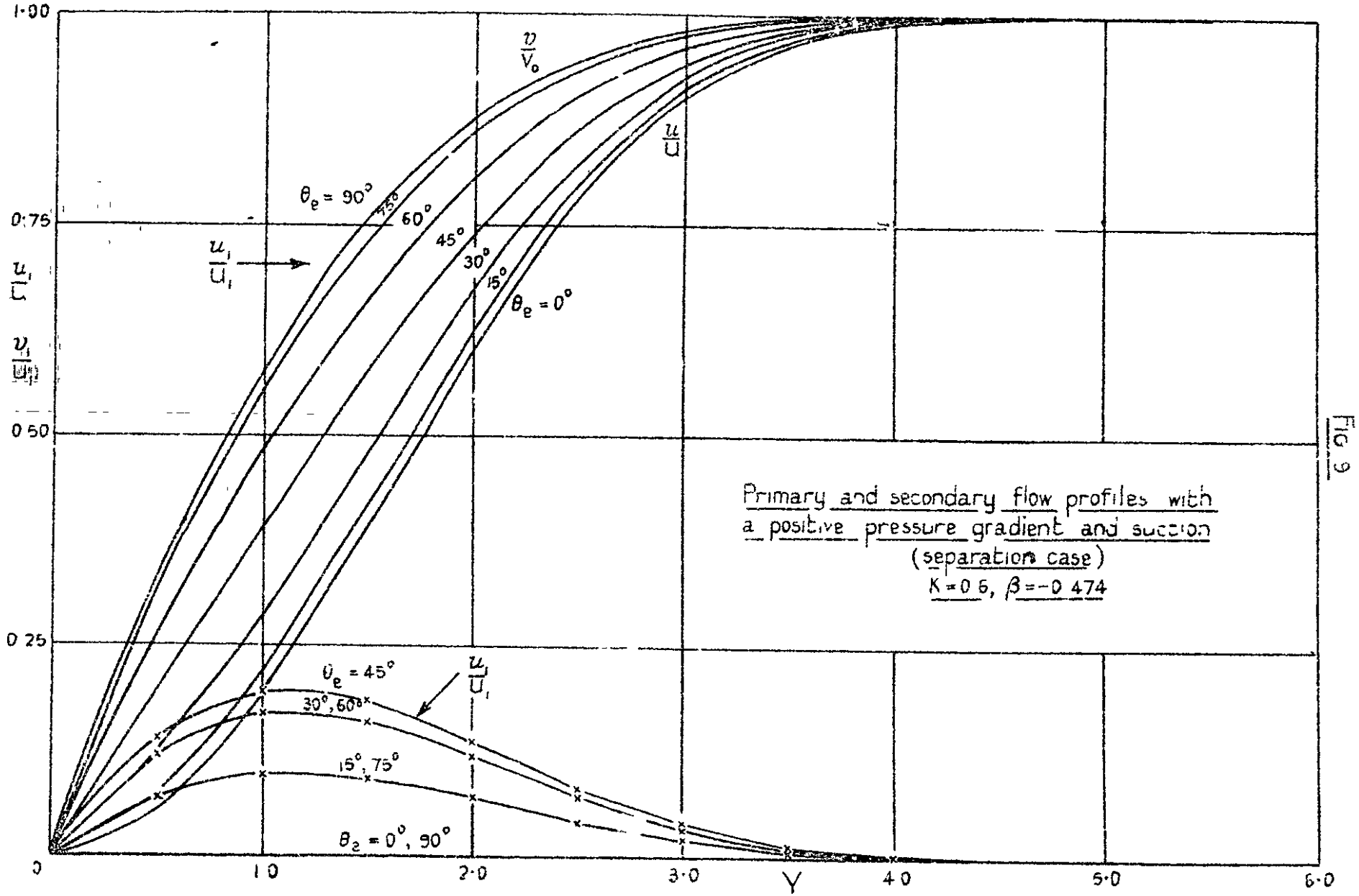

Primary and secondary flow profiles with a positive pressure gradient and suction (separation case)

K = 0·6, β = −0·474

Fig. 9

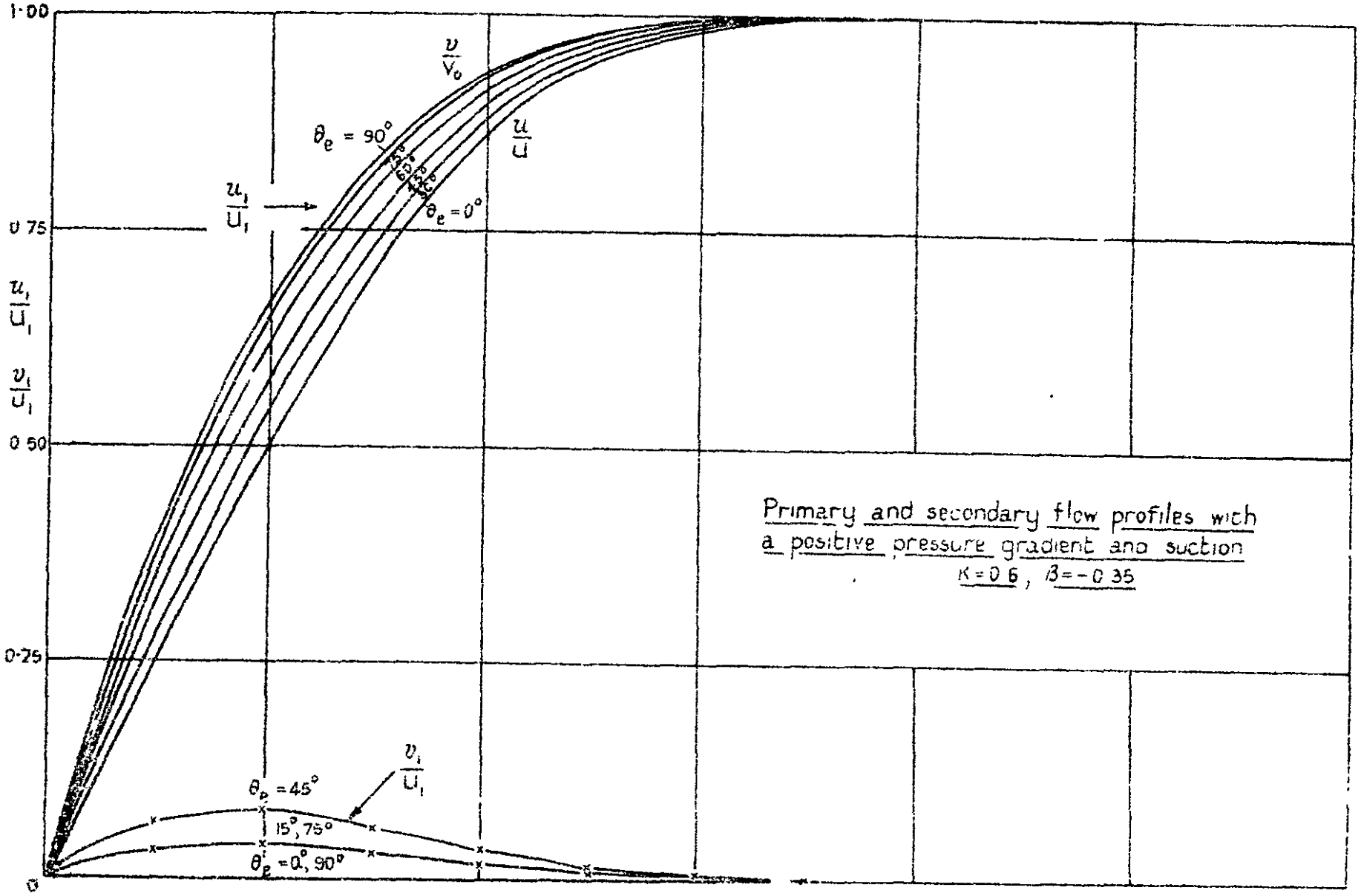

Primary and secondary flow profiles with a positive pressure gradient and suction
$K = 0.6$, $\beta = -0.35$

Fig 10

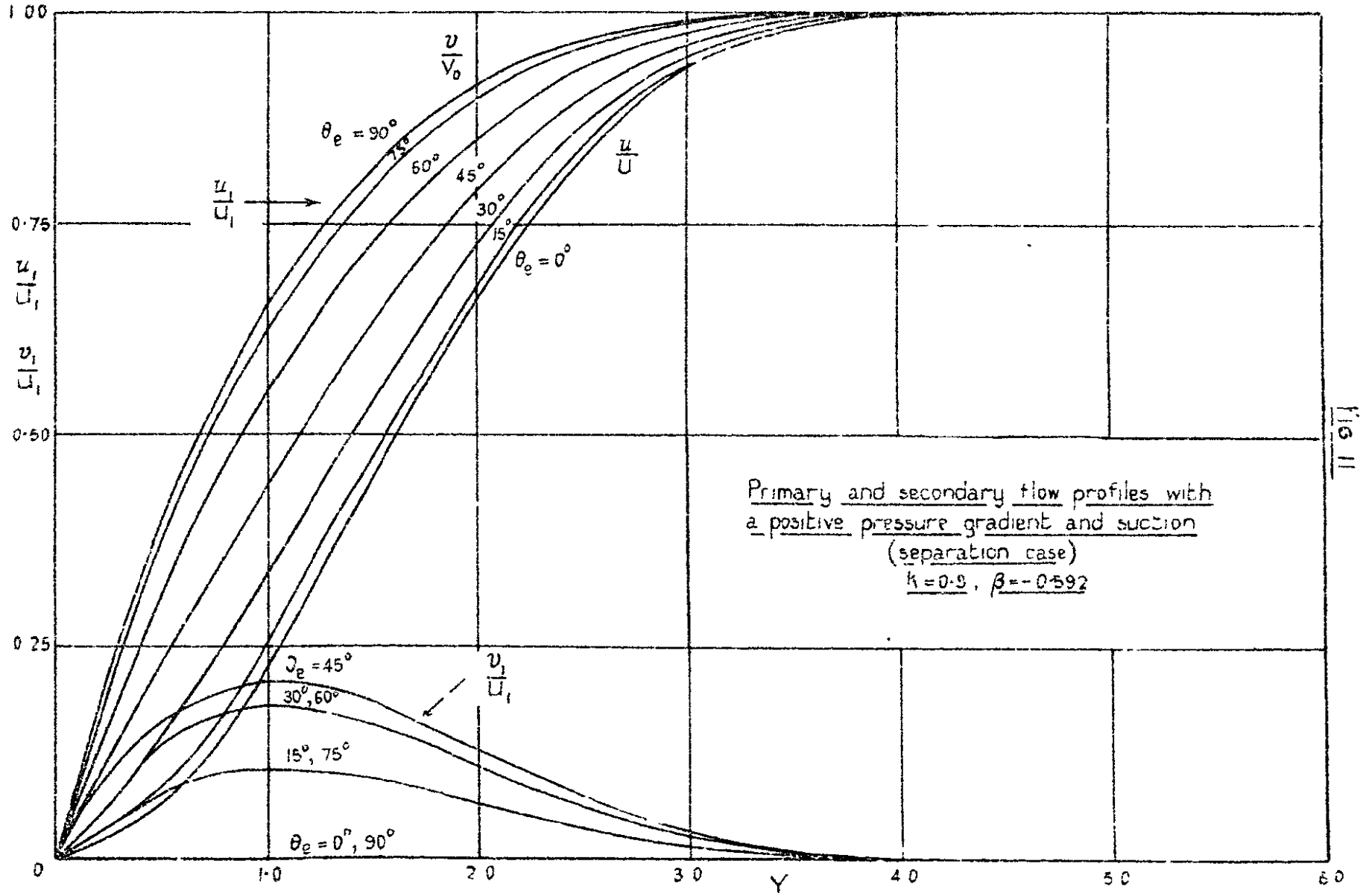

Primary and secondary flow profiles with a positive pressure gradient and suction (separation case)
$k = 0·9$, $\beta = -0·592$

Fig 11

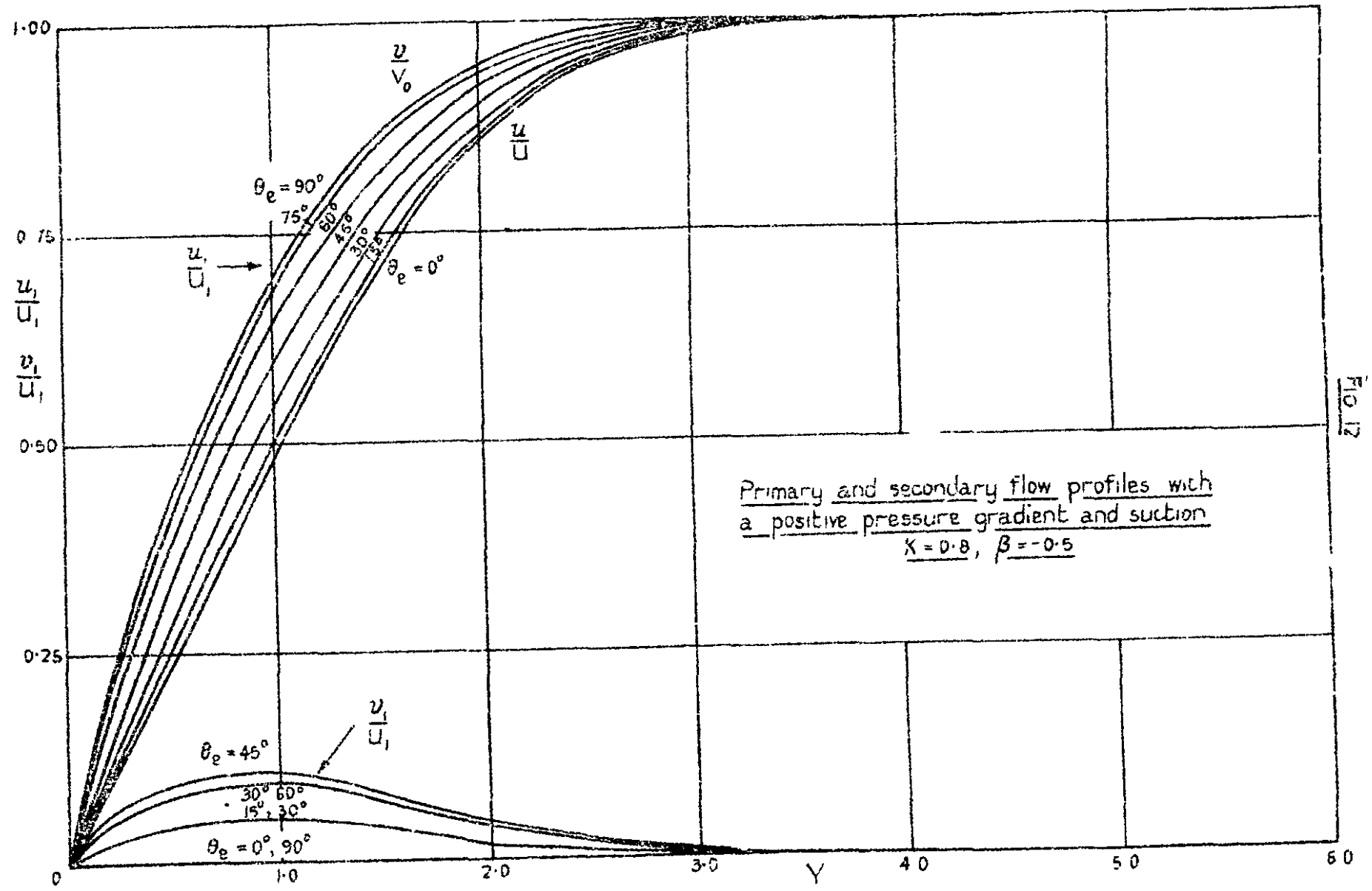
1·00
0·75
0·50
0·25
0
$\frac{u_1}{U_1}$
$\frac{v_1}{U_1}$
$\frac{v}{V_0}$
$\frac{u}{U}$
$\theta_e = 90°$
75°
60°
45°
30°
15°
$\theta_e = 0°$
$\frac{u_1}{U_1}$
$\frac{v_1}{U_1}$
$\theta_e = 45°$
30° 60°
15°, 30°
$\theta_e = 0°, 90°$
1·0
2·0
3·0
Y
4·0
5·0
6·0
Primary and secondary flow profiles with a positive pressure gradient and suction
$X = 0·8$, $\beta = -0·5$
Fig. 12

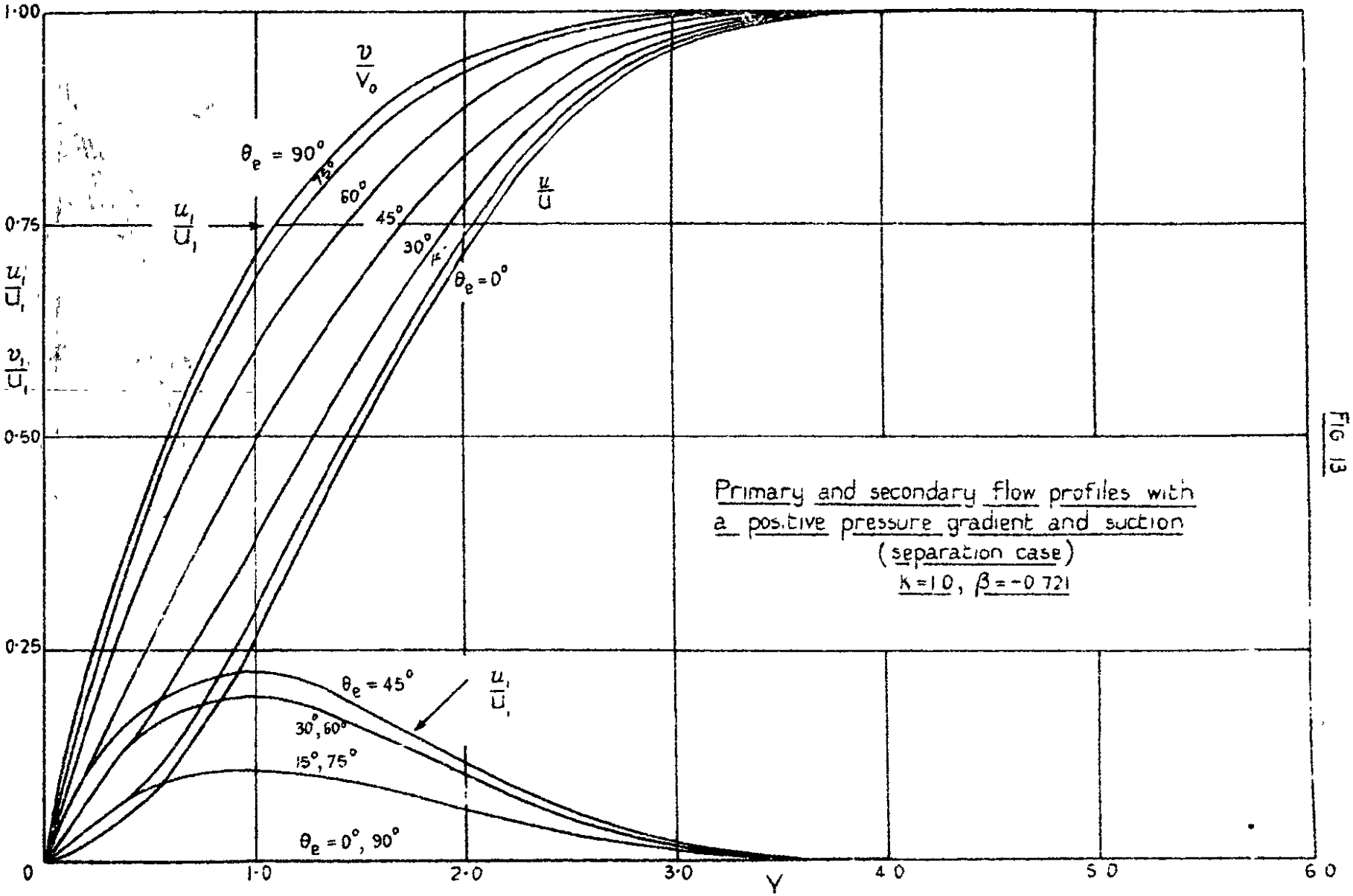
1·00
0·75
0·50
0·25
0
1·0
2·0
3·0
4·0
5·0
6·0
Y
$\frac{v}{V_o}$
$\frac{u}{U}$
$\frac{u_1}{U_1}$
$\frac{v_1}{U_1}$
$\theta_e = 90°$
75°
60°
45°
30°
$\theta_e = 0°$
$\theta_e = 45°$
30°, 60°
15°, 75°
$\theta_e = 0°, 90°$
Primary and secondary flow profiles with a positive pressure gradient and suction
(separation case)
K = 1·0, β = −0·721

FIG 13

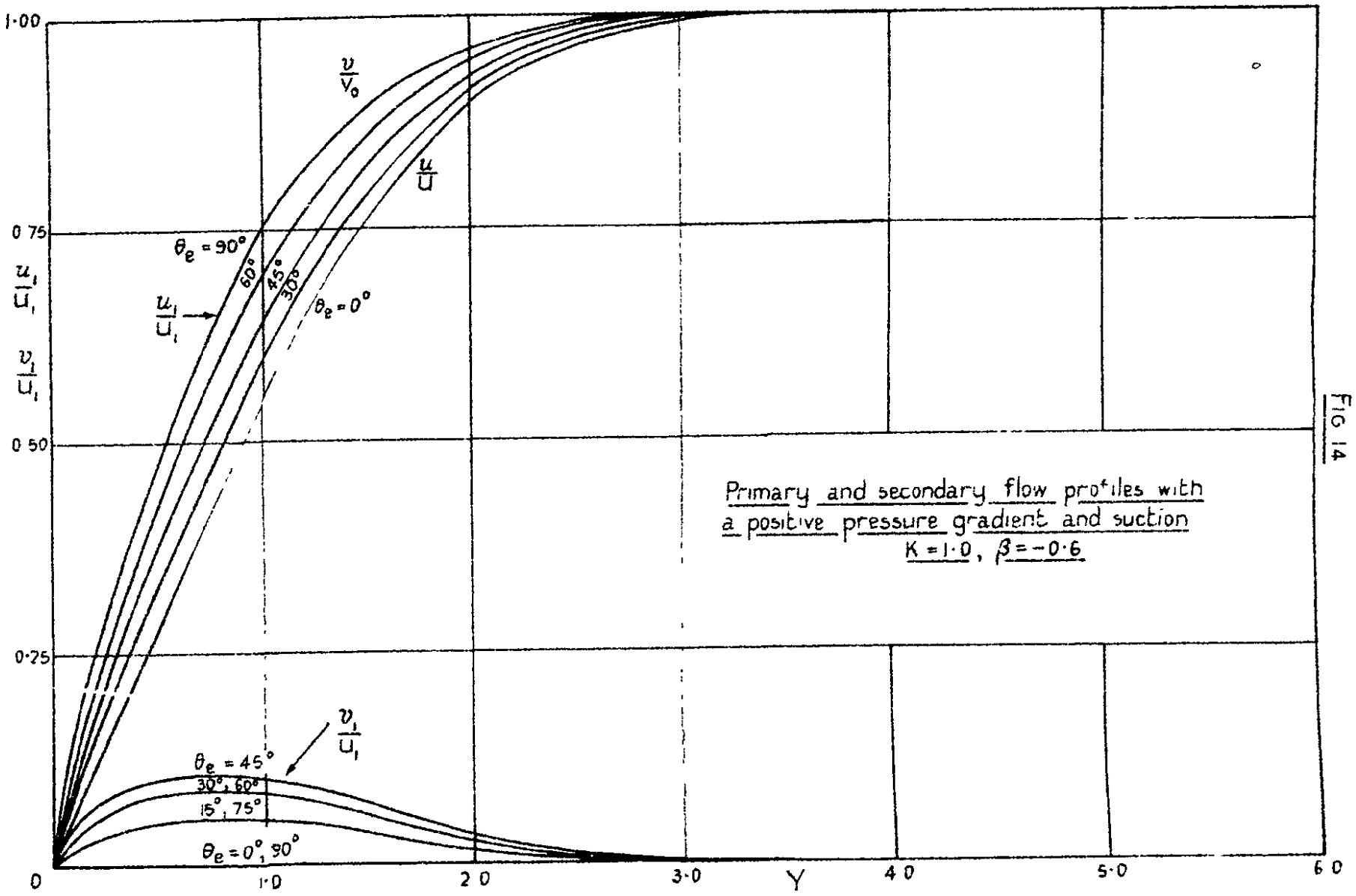

Primary and secondary flow profiles with a positive pressure gradient and suction
K = 1·0, $\beta = -0·6$

FIG 14

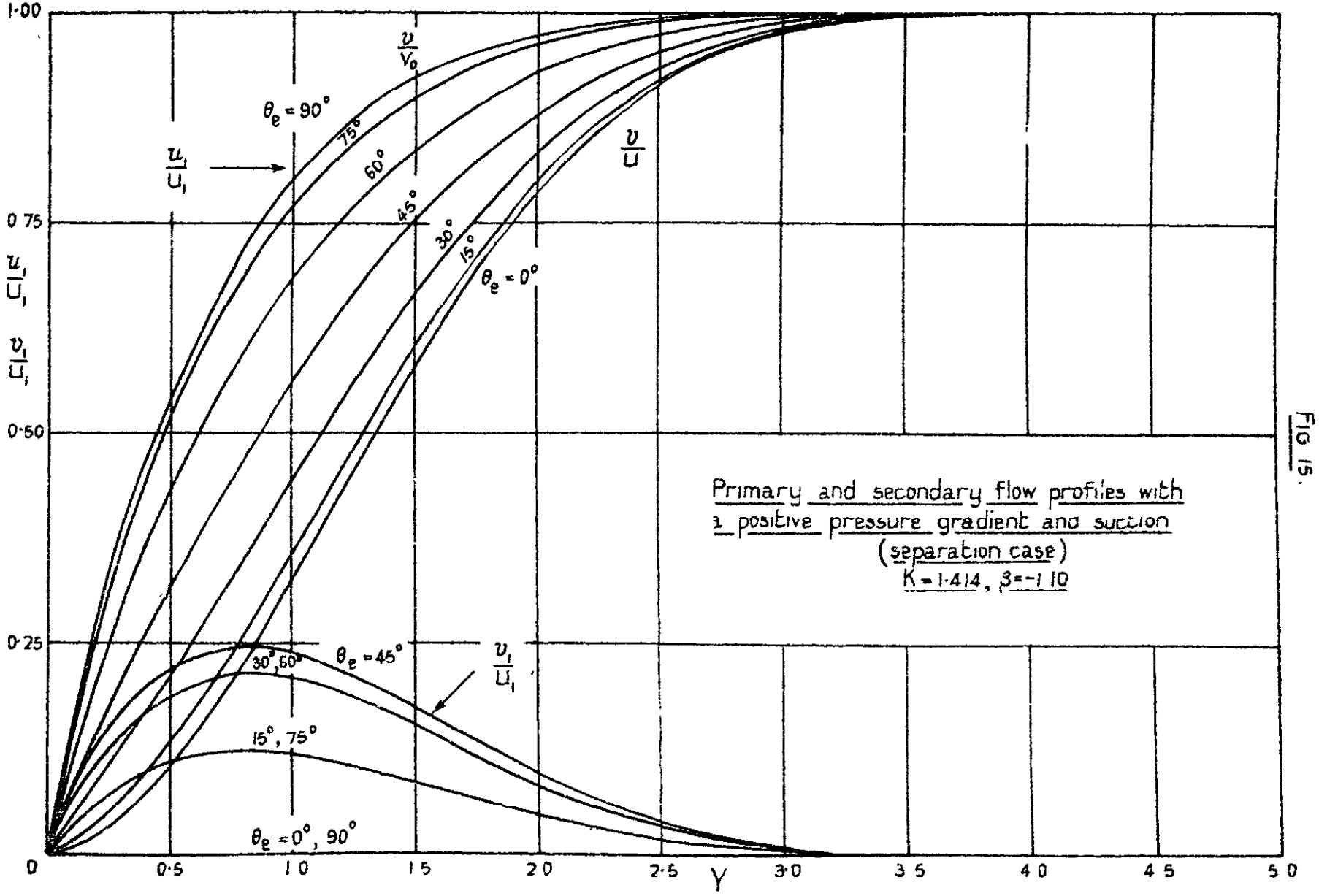
1·00
0·75
0·50
0·25
0
0·5
1·0
1·5
2·0
2·5
3·0
3·5
4·0
4·5
5·0
Y
$\frac{u_1}{U_1}$
$\frac{v_1}{U_1}$
$\frac{v}{V_0}$
$\frac{v}{U}$
$\theta_e = 90°$
75°
60°
45°
30°
15°
$\theta_e = 0°$
$\theta_e = 45°$
30°, 60°
15°, 75°
$\theta_e = 0°, 90°$
Primary and secondary flow profiles with a positive pressure gradient and suction (separation case)
K = 1·414, β = −1·10

Fig 15.

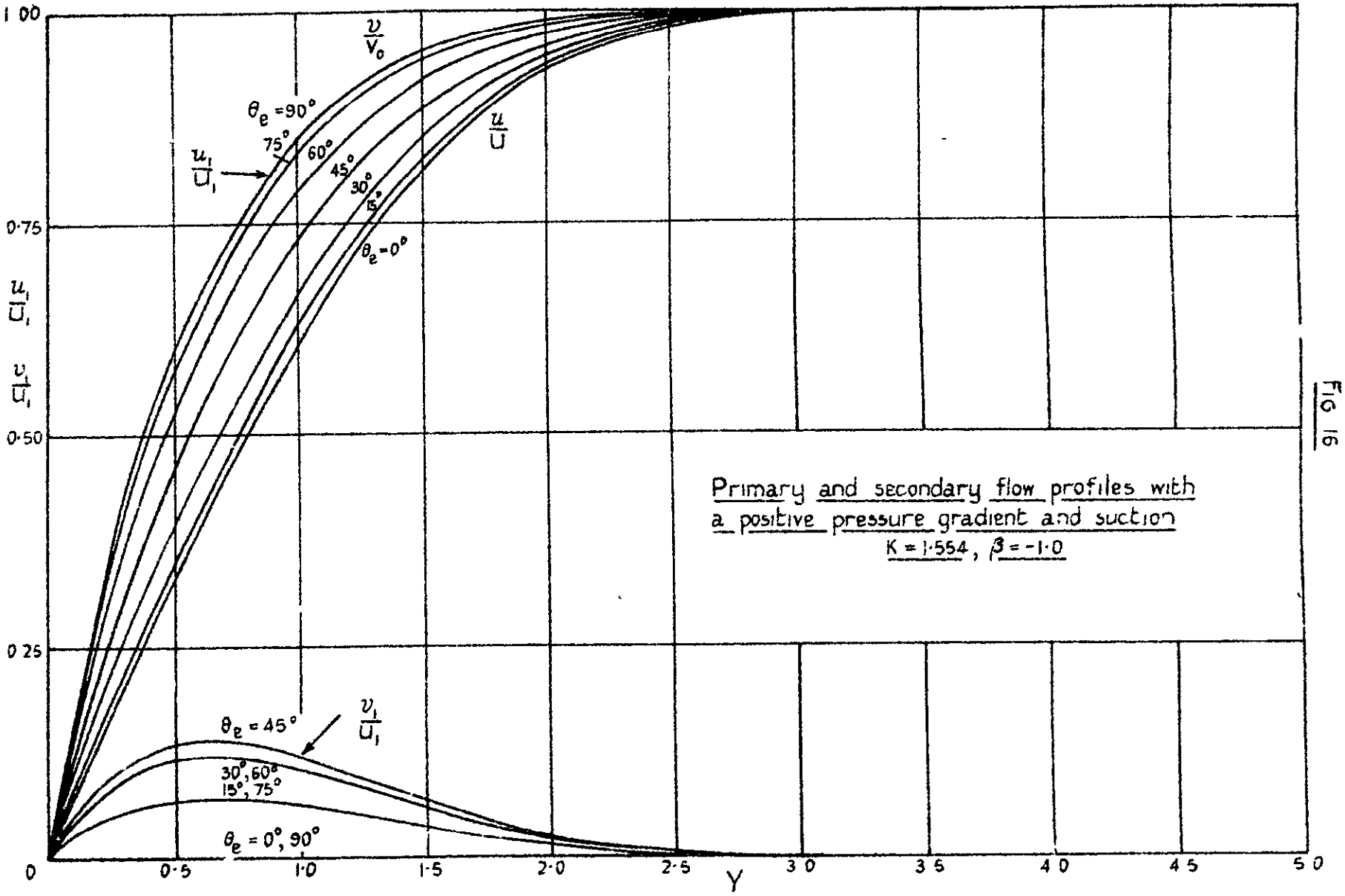
1·00
0·75
0·50
0·25
0
$\frac{u_1}{U_1}$
$\frac{v_1}{U_1}$
$\frac{v}{V_0}$
$\frac{u}{U}$
$\theta_e = 90°$
75°
60°
45°
30°
15°
$\theta_e = 0°$
$\frac{u_1}{U_1}$
$\frac{v_1}{U_1}$
$\theta_e = 45°$
30°, 60°
15°, 75°
$\theta_e = 0°, 90°$
0·5
1·0
1·5
2·0
2·5
3·0
3·5
4·0
4·5
5·0
Y
Primary and secondary flow profiles with a positive pressure gradient and suction
K = 1·554, β = -1·0

Fig 16

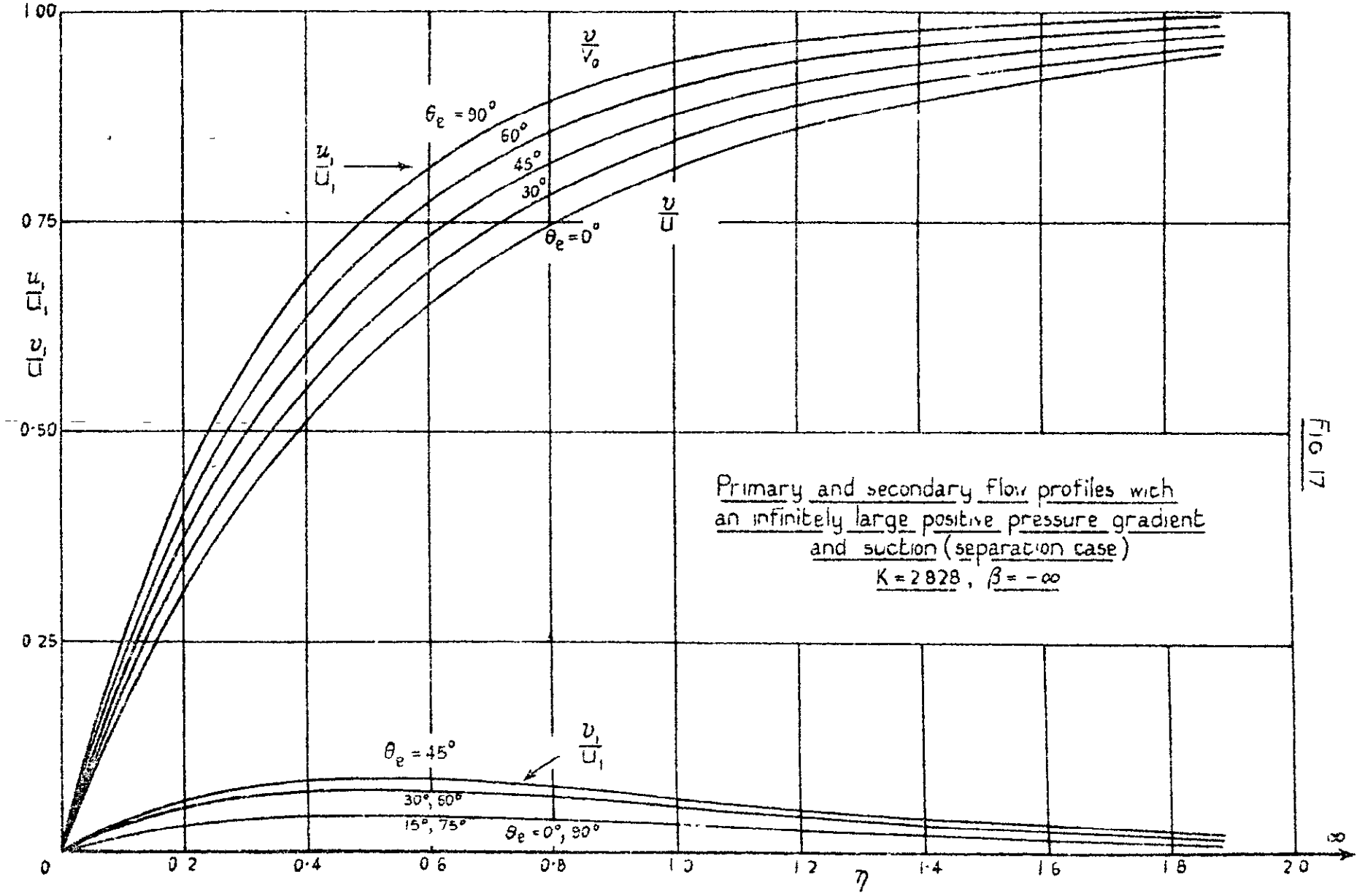
1·00
0·75
0·50
0·25
0
0·2
0·4
0·6
0·8
1·0
1·2
1·4
1·6
1·8
2·0
η
∞
u/U
v/U
v/v₀
u₁/U₁
v₁/U₁
θe = 90°
60°
45°
30°
θe = 0°
θe = 45°
30°, 60°
15°, 75°
θe = 0°, 90°
Primary and secondary flow profiles with an infinitely large positive pressure gradient and suction (separation case)
K = 2·828 , β = −∞

Fig 17

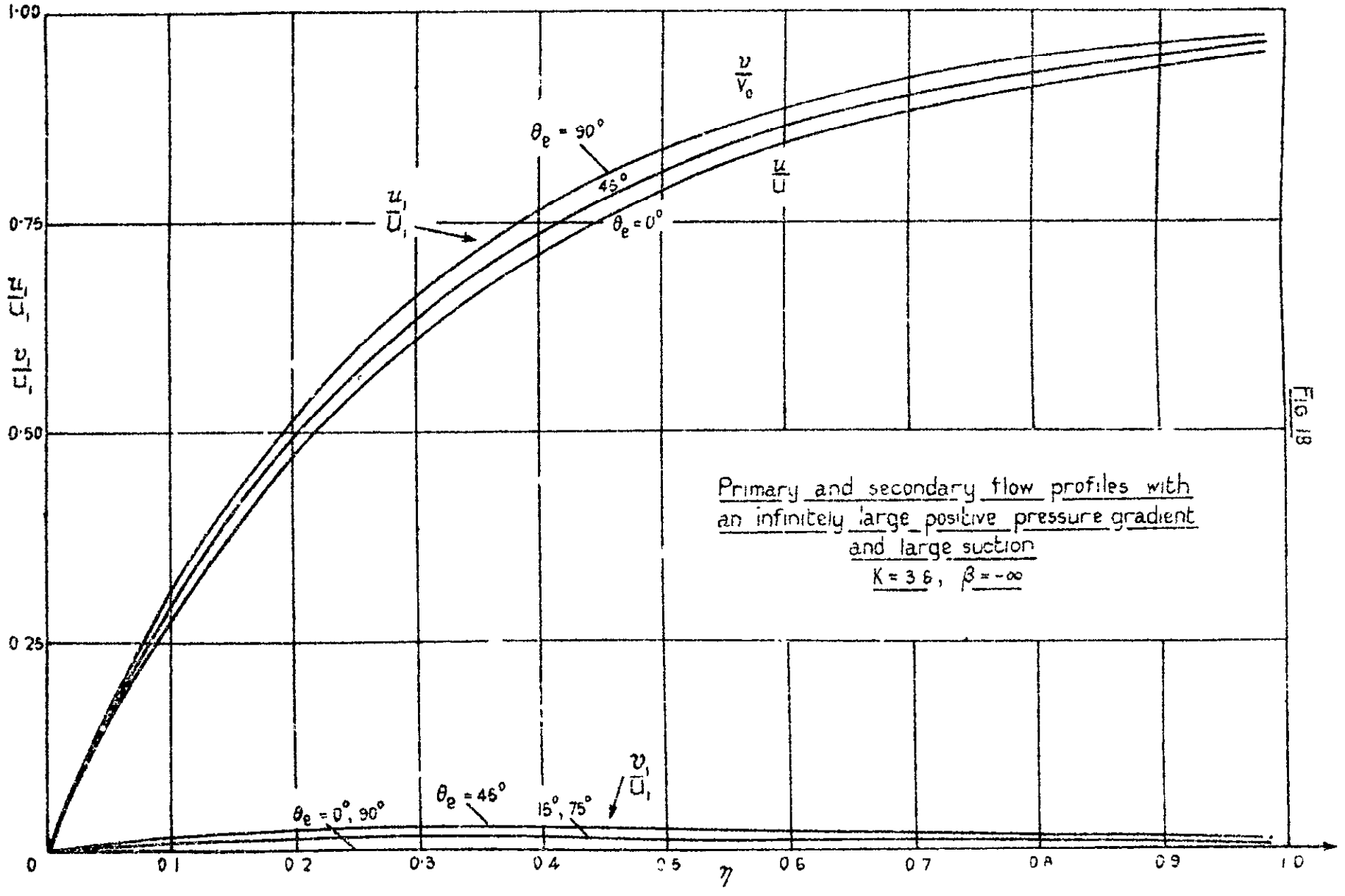
1·00
0·75
0·50
0 25
0
0 1
0 2
0·3
0 4
0 5
0 6
0 7
0 A
0 9
1 0
η
u/U, v/U
u₁/U₁
v₁/U₁
v/V₀
u/U
θe = 90°
45°
θe = 0°
θe = 0°, 90°
θe = 45°
15°, 75°
Primary and secondary flow profiles with an infinitely large positive pressure gradient and large suction
K = 3 6, β = -∞
Fig 18

FIG 19

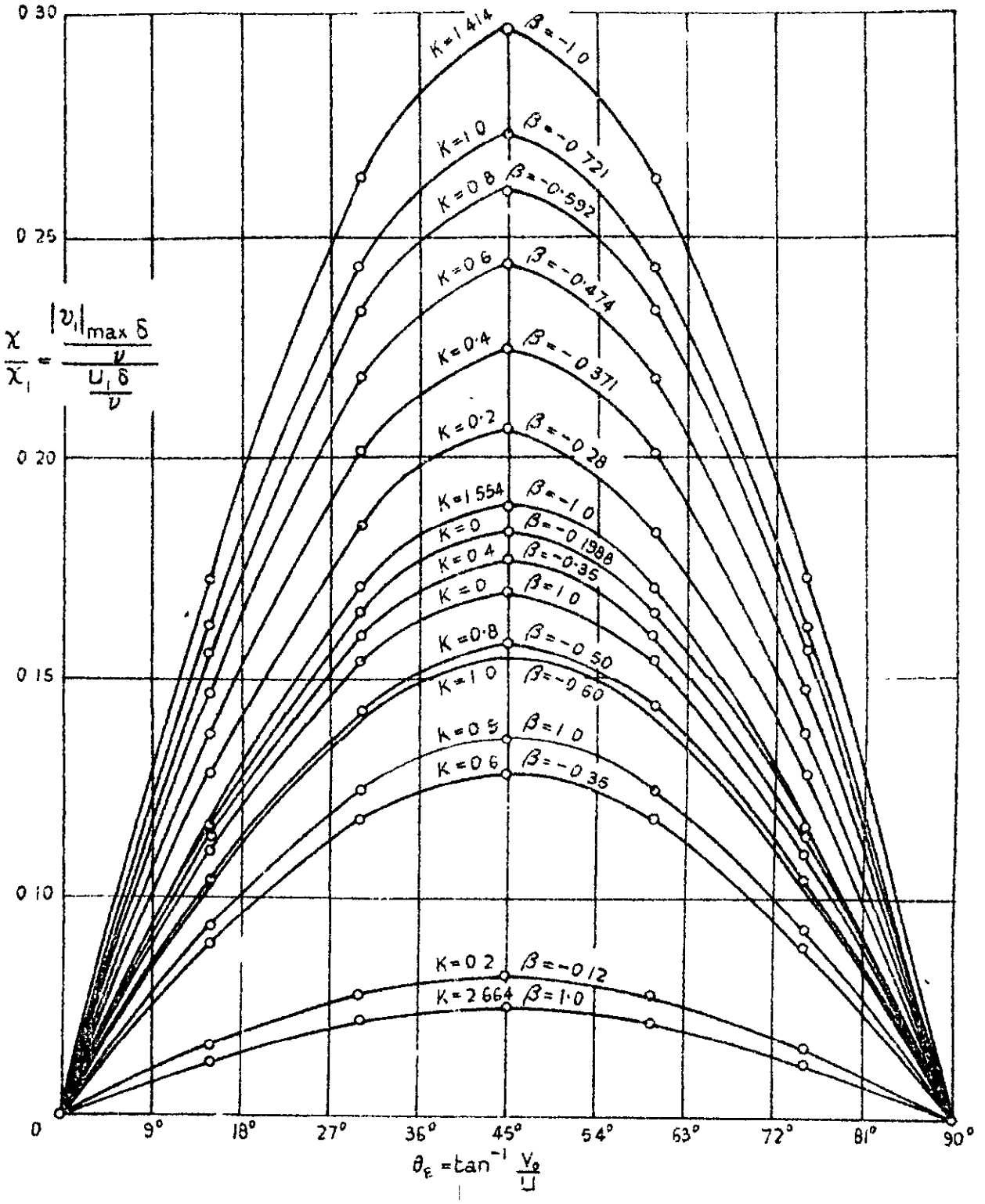

Variation of the ratio of the secondary flow Reynolds number to the primary flow Reynolds number with the inclination of the edge streamline to the chordwise direction

C.P. No. 295
(18,181)
A.R.C. Technical Report

Printed and published by
HER MAJESTY'S STATIONERY OFFICE

To be purchased from
York House, Kingsway, London W C 2
423 Oxford Street, London W.1
P.O. Box 569, London S E 1
13A Castle Street, Edinburgh 2
109 St. Mary Street, Cardiff
39 King Street, Manchester 2
Tower Lane, Bristol 1
2 Edmund Street, Birmingham 3
80 Chichester Street, Belfast
or through any bookseller

Printed in Great Britain

S.O Code No. 23-9009-95

C.P. No. 295